*Revised manuscript with no changes marked

Geochemistry of deep Manihiki Plateau crust: Implications for compositional diversity of large igneous provinces in the Western Pacific and their genetic link

Roman Golowin[1], Maxim Portnyagin[1,2*], Kaj Hoernle[1,3], Folkmar Hauff[1], Reinhard Werner[1] and Dieter Garbe-Schönberg[3]

[1]GEOMAR Helmholtz Centre for Ocean Research Kiel, Wischhofstrasse 1-3, 24118, Kiel, Germany

[2]V.I.Vernadsky Institute of Geochemistry and Analytical Chemistry, Kosigin str. 19, 119991, Moscow, Russia

[3]Institut für Geowissenschaften, Christian-Albrechts-Universität zu Kiel, Ludewig-Meyn-Strasse 10, 24118 Kiel, Germany

* Corresponding author (mportnyagin@geomar.de)

Revised manuscript submitted to *Chemical Geology*

Abstract

Geochemical studies revealed two major high- and low-Ti magmatic series composing the Manihiki Plateau in the Western Pacific. Here we report new geochemical data on major and trace element and Sr-Nd-Pb isotope compositions. The rocks belong to the previously rarely sampled high-Ti Manihiki series and represent a section of deep crust of the plateau. The rocks were collected by remotely operated vehicle ROV Kiel6000 during R/V SONNE SO225 expedition from a tectonic block at a stretched and faulted boundary between the Northern and Western Manihiki sub-plateaus. The dataset is accompanied by additional data on samples obtained by dredging during the same cruise. Judging from the age of stratigraphically higher lavas most samples appear ≥125 Ma old. They comprise fully crystalline microdolerites, aphyric and *Ol*-*Px*-*Pl*-phyric basalts and breccias metamorphosed under amphibolite and greenschist facies with peak metamorphic conditions 636-677 ^{o}C and 2.0-2.7 kbar. A single sample of hornblende gabbro was also recovered and likely represents a late stage intrusion. Despite strong metamorphism, the samples from the ROV profile reveal only minor to moderate chemical alteration and their initial compositions are well preserved. The rocks are relatively primitive with MgO up to 13 wt%, range from enriched to depleted in LREE (La_N/Sm_N=0.7-1.1), exhibit variable but mostly depleted Nb contents (Nb/Nb*=0.8-1.3) and display only a narrow range in isotope compositions with strong EM1 signature (εNd(t)=1.8-3.6, $^{206}Pb/^{204}Pb$ (t)=17.9-18.1, $^{207}Pb/^{204}Pb$ (t)=15.49-15.53 , $^{208}Pb/^{204}Pb$ (t)=38.08-38.42). The parental magmas are interpreted to originate from a thermochemical plume with a potential mantle temperature >1460^{o}C. The trace element and isotope EM1 signature of the high-Ti rocks reflects the presence of recycled lower continental crust material or re-fertilized subcontinental lithospheric mantle in the plume source. A highly refractory mantle was the primary source of the low-Ti basalts and could also contribute to the origin of high-Ti basalts. On average a more depleted mantle source for the Manihiki rocks can explain ~30% lower crustal thickness of this plateau compared to Ontong Java Plateau, which was mainly formed by melting of similarly hot but more fertile mantle. The presently available data suggest that the sources of Ontong Java and Manihiki Plateaus were compositionally different and could represent two large domains of a single plume or two contemporaneous but separate plumes.

Keywords: LIP, Manihiki Plateau, Ontong Java, Sr-Nd-Pb isotopes, trace elements, mantle components, depleted mantle, enriched mantle one, EM1, recycling, subcontinental lithospheric mantle, SCLM

Highlights:

- First data on the composition of deep crust and primitive rocks of high-Ti magmatic series of Manihiki Plateau;
- High potential mantle temperature for Manihiki sources (>1460°C) suggests a lower mantle plume origin;
- EM1 signature in Manihiki basalts could originate from recycled lower continental crust or re-fertilized subcontinental lithospheric mantle;
- The presence of refractory mantle in the Manihiki plume explains the lower productivity of mantle melting and 30% lower crustal thickness compared to OJP;
- Manihiki and OJP could have been formed from a spatially, geochemically zoned plume or by two spatially separated mantle plumes.

1. Introduction

The Ontong Java, Manihiki and Hikurangi Plateaus in the Western Pacific, together covering >1% of the earth's surface, were emplaced at c. 125 Ma as one single Ontong Java Nui "super" plateau and thus are likely to represent the largest magmatic event in the Phanerozoic (Taylor, 2006; Davy et al., 2008; Hoernle et al., 2010; Timm et al., 2011; Chandler et al., 2012; Hochmuth et al., 2015). The origin of the magmatic event is still controversial. The prevailing hypothesis invokes mantle plume head melting (Mahoney, Spencer, 1991; Larson, 1991a,b; 1997; Hoernle et al., 2010). Impact origin (Rogers, 1982; Ingle, Coffin, 2004) and melting of eclogite under a super-fast spreading ridge (Korenaga, 2005) have also been proposed. The key evidence for the former existence of a single plateau, before it was broken apart and dispersed by plate movements, comes from recent palaeo-tectonic reconstructions (Taylor, 2006; Chandler et al., 2012), geophysical data (Hochmuth et al., 2015), and ages and compositions of volcanic rocks comprising these plateaus (Hoernle et al., 2010; Timm et al., 2011). Whereas the joint origin of the Manihiki and Hikurangi Plateaus and their later separation by the spreading at the Osborn Trough is well justified by the Western Pacific plate kinematics (Billen and Stock, 2000; Davy et al., 2008), the tectonic relationships between the Ontong Java and Manihiki Plateaus are less certain (Larson et al., 1997; Taylor, 2006; Chandler et al., 2012; Hochmuth et al., 2015).

Although the similarity of rock compositions and their ages is commonly cited to advocate the conjunctive origin of the Ontong Java, Manihiki and Hikurangi plateaus, the existing data indicate significant heterogeneity of the rock compositions within each plateau and likely a significant time interval for their formation. The compositions of the Ontong Java rocks have been studied through deep-sea drilling at 10 sites in the plateau and neighbouring Nauru and East Mariana basins and extensive sampling of subaerially exposed rocks on Malaita and Santa Isabel, Solomon Islands (Manohey et al., 1993; Tejada et al., 1996; 2004; 2002; Fitton and Godard, 2004). The Ontong Java Plateau rocks have been divided into three groups based on their major and trace element compositions: Kwaimbaita evolved tholeiites, dominant rock group; Kroenke primitive tholeiites with similar Sr-Nd-Pb isotopic composition to Kwaimbaita lavas; and Singgalo enriched tholeiites with enriched incompatible element contents and more enriched Sr-Nd-Pb isotopic compositions than the Kwaimbaita and Kroenke groups (e.g., Mahoney et al., 1993; Tejada et al., 2002; 2004; Fitton and Godard, 2004). A distinctive feature of the Ontong Java rocks is the relatively narrow range of Sr-Nd-Pb isotope compositions of the Kwaimbaita-Kroenke and Singgalo groups.The ages of Ontong Java rocks indicate a major volcanic pulse at ~122 Ma followed by a less volumetric event at ~90Ma (e.g. Tejada et al., 2002). Scarce data of Hikurangi basement rocks indicate ages scattering from 96 to 118 Ma, broadly between the two magmatic pulses at Ontong Java, but trace element and Sr-Nd-Pb isotopic compositions are very similar to the Kwaimbaita group (Hoernle et al., 2010). Reported ages of Manihiki rocks range from 116 to 125 Ma (Hoernle et al., 2010; Timm et al., 2011) and thus span the earliest stage of both Ontong Java and Hikurangi plateau formation. The reported compositions of Manihiki rocks are, however, more scattered compared to Ontong Java and Hikurangi. Many rocks sampled in deep canyons cutting the Manihiki plateau are strongly depleted in moderately incompatible elements ("low-Ti" group after Timm et al. (2011)) and have spoon-shaped normalized trace element pattern, exotic for intraplate oceanic rocks. The spoon-shaped patterns were interpreted to originate from re-melting of previously depleted and metasomatized mantle (Ingle et al., 2007; Golowin et al., 2017a,b), which is proposed but not necessarily present in the source of Ontong Java. The high-Ti group of Manihiki rocks was sampled by a 35 m long section at DSDP site 317A and a few dredges in the northern part of the plateau (Hoernle et al., 2010; Timm et al., 2011). These high-Ti Manihiki rocks are more similar to OJP rocks in incompatible trace element compositions but have distinctive EM1-like isotope signatures. The scarcity of data on the composition of basement rocks from the Manihiki and Hikurangi plateaus leaves much room for various interpretations of their genesis, either in connection with Ontong Java or not. None of the models, however, can be fully excluded by the paleotectonic reconstructions (Larsen et al., 1997; Taylor, 2006).

In this paper we report new data on the composition of deep crust of the Manihiki plateau, which was sampled with the ROV Kiel 6000 and dredging during the R/V Sonne expedition SO225. We also report new high-precision Pb isotope data on rocks from DSDP Site 317A Manihiki rocks. The compositions allow better characterization of the high Ti-rock suite and show a wide spatial distribution of these lavas in the Manihiki Plateau basement. We show that, although these rocks were metamorphosed under greenschist to amphibolite facies, their primary compositions are well preserved. The new samples extend the range of known high-Ti Manihiki rocks to higher MgO contents, allowing direct comparison with Kroenke lavas and evaluation of mantle melting conditions. Despite close similarity in major and trace element, as well as isotopic, composition with Ontong Java and Hikurangi rocks, the Manihiki high-Ti rocks have distinctive Sr-Nd-Pb isotope compositions, implying a distinct enriched component in their source, different from the one in the source of Singgalo lavas. The data is used to discuss the proposed origin of Ontong Java and Manihiki Plateaus by melting of a single mantle plume.

2. Geological framework and samples studied

The Manihiki Plateau is located in the western Pacific ~ 700 km NE of Samoa and occupies an area of 800,000 km^2 (Fig. 1). Most parts of the plateau are located in water depths between 3500 and 5000 m.b.s.l. and are covered by up to 1 km of sediments. The main part of the plateau is thought to be formed in the late Cretaceous ~116-125 Ma due to voluminous plume-related volcanism (Ingle et al., 2007; Hoernle et al., 2010; Timm et al., 2011). The plume-related origin is reflected by anomalously (up to 20 km) thick oceanic lithosphere (yet not as thick as under Ontong Java), and the presence of a prominent high-velocity zone, likely olivine ± pyroxene cumulates, at the crust-mantle boundary (Hochmuth et al., 2015). The plateau has been strongly deformed. Its northern and eastern margins are prominently sheared and represented by steep scarps. The western and southern margins are rifted and stretched. The inner parts of the plateau are also fragmented (Winterer et al., 1974; Hochmuth et al., 2015). The most prominent intra-plateau features are deep pull-apart graben-like basins, Danger Island Trough and Suvorov Trough, which divide the Manihiki Plateau into the High, Western and North Plateaus (Winterer et al., 1974; Nakanishi et al., 2015) (Fig. 1). The strong tectonic fragmentation provides an excellent opportunity to sample some inner parts of the Manihiki plateau without drilling, as demonstrated previously (Ingle et al., 2007; Timm et al., 2011; Golowin et al., 2017a,b).

The rocks studied here were recovered using remotely operated vehicle (ROV) Kiel 6000 and dredging during the R/V Sonne expedition SO225 (Werner et al., 2013). Sampling with ROV was performed at the boundary between the North and Western Plateaus (Fig. 1, 2). The boundary is expressed in this area by a series of NW-SE elongated troughs, small ridges and larger crustal blocks and was likely formed by post-emplacement rifting and stretching of the Manihiki crust driven by plate tectonic processes (Hochmuth et al., 2015). The ROV sampling targeted a c. 10 km long triangular, steeply-walled crustal block (Fig. 2). The block consists of three ridges that converge at the summit. The curvature in the deeper parts of the ridges is likely of tectonic origin and could reflect anti-clock-wise rotation during emplacement. Relatively fresh 125 ± 2.1Ma rocks were dredged at the summit during SO193 expedition (sample SO193-DR46-1) (Timm et al., 2011).

A continuous sampling profile was made in two dives (ROV3 and ROV4) on SO225 across the south-west facing slope of the block over a depth interval of 4600 and 3300 m.b.s.l. (Fig. 2b). The slope had a stair-case profile and in most parts appeared as a relatively continuous outcrop with “pillowed” surface partly covered with unconsolidated pelagic sediments (Fig. 2c). In some parts the surface is cut by slope parallel fractures suggesting normal faulting. Rock debris occurred typically as slope talus and comprised small rock fragments and large angular blocks of up to 3 m across (Fig. 2d). The “pillowed” surface of the sea floor appeared to be made by up to 15 cm thick Mn crusts covering rock outcrops and also cementing rock debris. The thick encrustations made it impossible to sample in-situ rocks by either ROV jaws or chisel. The samples collected were loose rock fragments from debris and likely originated from the nearby outcrops upslope. Of the 28 samples collected, 20 were magmatic / metamorphic rocks, which we studied geochemically. Their coordinates and sampling depth are listed in Supplementary table 1. The remaining samples were breccias composed of angular basaltic fragments cemented by mudstone and consolidated pelagic sediments. Illustrated on-board description of the samples can be found in Werner et al (2013).

In addition, we studied several samples obtained by dredging during SO225. These samples belong to the same geochemical type as ROV samples and were collected from the northern margin of the High Plateau, in the middle part of the Danger Island Trough and in the Suvorov Trough (Fig. 1, Supplementary table 1). Most of these rocks were highly altered and thus provide limited useful petrogenetic geochemical information. They are reported here for the sake of comparison with the ROV samples.

3. Methods

All rocks samples were studied petrographically in thin section. Selected samples were investigated by electron imaging and for composition of rock-forming minerals with electron microprobe at GEOMAR. Major elements in bulk rock samples were obtained by XRF (Hamburg University) and ICP-MS (Institute of Earth Sciences at Kiel University). Sr, Nd and Pb (double spike) isotope compositions were determined by TIMS (GEOMAR). Detailed description of the analytical techniques can be found in Supplementary methods. The analytical data are presented in Supplementary tables 1-4. In addition to SO225 rock samples, we report new high-precision Pb isotope data for 5 samples recovered at the DSDP Site 317A.

Conventional Pb along with high precision Sr-Nd isotope data for these samples were previously reported by Hoernle et al. (2010).

4. Results

4.1. Petrographic rock types

All ROV samples are metamorphosed under greenschist to amphibolite facies and range from rocks with minor metamorphic overprint and well preserved magmatic textures to greenschists and amphibolites with nearly completely destroyed primary textures (Fig. 3). Most rocks from the lower part of the ROV profile are massive microdolerites with characteristic ophitic texture (Fig. 3a). In the upper part, the rock varieties are more diverse and their textures tend to be more fine-grained. Along with dolerites, vesicular aphyric and massive *Ol*±*Pl*±*Cpx* phyric basalts were identified. Sample ROV3-11 has distinctively fine-grained texture (Fig. 3d) and revealed different chemical composition. Greenschist (sample ROV4-14) was also collected from the upper part of the ROV profile, likely representing strongly sheared and fully metamorphosed basaltic protolith (Fig. 3g).

Except rare relics of Cr-diopside in the sample of magmatic breccia ROV4-1, olivine and pyroxene in the rocks were not preserved and replaced by chlorite and amphibole. Plagioclase is commonly pierced by acicular actinolite and was likely recrystallized during metamorphism. Electron microprobe survey of representative sample of microdolerite ROV3-6 revealed that the rock is mostly composed of normally zoned plagioclase laths ranging from $An_{70\text{-}74}$ in cores to $An_{42\text{-}61}$ at rims, acicular magnesio-ferri-hornblende and granular actinolite of characteristic low-Al and low-Ti composition (Fig. 3 a,b, Fig. 4; Supplementary table 3). Accessory minerals in the sample are ilmenite, apatite, titanite (typically forming wide fringe around ilmenite) and zircon occurring as micron-sized inclusions in titanite and ilmenite (Fig. 3b). The mineral assemblage is not representative of magmatic equilibria and likely represents a later metamorphic overprint. The paragenesis of acicular hornblende intergrown with plagioclase rims in this sample indicates peak metamorphic conditions at T=636-677 °C and P= 2.0-2.7 kbar as estimated from reaction edenite + albite = richterite + anorthite (Holland and Blundy, 1994). Judging from petrographic observations similar metamorphic changes are typical for most rocks studied.

Previously studied and dated sample SO193-DR46-1 from the top of the tectonic seamount (Timm et al., 2011) is a fully crystallized olivine dolerite with well-preserved magmatic texture composed of plagioclase, two pyroxenes and olivine (Fig. 3h). Texturally this sample is similar to metadolerites sampled by ROV but has less metamorphic overprint, which is mostly developed along fractures and reflects localized high-T fluid-rock interaction.

Sample ROV3-4, medium to coarse *Hbl*-gabbro, is distinct from other samples (Fig. 3e). The rock is mostly composed by partly altered idiomorphic up to 1 cm-long amphibole of Ti-rich pargasite, magnesio-hastingsite and ferri-sadanagaite composition and granular plagioclase $An_{39\text{-}53}$ in cores and $An_{13\text{-}29}$ at rims (Supplementary table 3, Figs. 3e-f, 4). Titanite, ilmenite, magnetite, apatite, quartz, zircon and rutile are also present. The conditions of equilibria estimated for plagioclase cores and relic amphibole range from T=872-877 °C and P=1.6-1.9 kbar for amphibole rims to T=830-845 °C and P=3.4-4.5 kbar for amphibole cores (Holland and Blundy, 1994). Secondary alteration is expressed in patchy albitization of plagioclase and by the occurrence of actinolite and epidote along fractures in primary amphibole and granular chlorite.

Samples dredged at sites SO225-DR8, -DR9, -DR21 and -DR23 on the flanks of the Central Danger Island and the Suvorov Troughs (Fig. 1) are variably vesicular *Ol*±*Cpx*±*Pl* basalts. The rocks are strongly altered under zeolite facies and contain abundant carbonates, zeolites and minerals of chlorite-group.

4.2. Bulk rock compositions

4.2.1. Effects of post-magmatic alteration

Weight losses on ignition (LOI) are typically measured and used to quantify overall degree of rock alteration. Some compositional parameters of SO225 rocks and previously published Manihiki compositions are plotted against LOI in Fig. 5. The LOI for published Manihiki samples range from <1 wt% up to 13 wt%. ROV samples revealed moderate LOI in the range of 0.86-3.16 wt%. Dredged samples contain more volatiles in the range of 6.2-7.39 wt%. Judging from the general systematics, significant changes in major and trace element compositions occur at LOI ~ 5 wt%. Rocks with LOI>5 wt% tend to have low MgO, MnO and very high $FeO_t/MnO>100$, which is beyond the range of primitive basalts (FeO_t/MnO ~30-100; Herzberg et al., 2010). They are strongly enriched in K_2O, as well as U, Rb, Cs and other elements prone to seafloor alteration (e.g., Hart and Staudigel, 1982), and also display pronounced negative Ce anomaly ($Ce/Ce^* < 0.8$, where $Ce/Ce^* = Ce_n/(La_n \times Nd_n)^{0.5}$ calculated for primitive mantle-normalized concentrations) in mantle-normalized REE patterns. These compositional changes cannot be explained by fractional crystallization processes but are typical for submarine alteration, particularly at seamounts and submarine plateaus (e.g., Masuda and Nagasawa, 1975; Fodor et al., 1987; Le Roex et al., 2010; Tejada et al., 2016; Frisby et al., 2016). Along with the uptake of volatile components (H_2O, CO_2) and alkalis, a characteristic feature of this type of submarine alteration is the uptake of REEs but not Ce, because Ce^{4+} is not as easily mobilized as the trivalent REEs under oxidizing conditions (e.g., Le Roex et al., 2010 and references therein). Our data testify that Mg and Mn are lost from rocks during this type of submarine alteration.

Following these empirical observations, we consider rocks with LOI>5 wt% as highly altered (similarly to conclusions of Le Roex et al., 2010) and, except for the least mobile elements in these rocks, such as Al, Ti, Th, Zr, Nb and Ta (e.g. Pearce and Norry, 1979), do not use their compositions for genetic interpretations. All dredged samples are considered to be highly altered. The ROV samples are considered to be only "moderately" altered, despite mineralogical evidence of strong high-*T* metamorphic modification, because they do not show abnormal geochemical characteristics.

4.2.2. Major elements and compatible trace elements

The majority of the recovered ROV samples have tholeiitic (SiO_2 = 50-54 wt%, N_2O+K_2O = 1.7-3.1 wt%) basaltic compositions (Supplementary table 1; Fig. 6). MgO content ranges from 6.6 to 13 wt% and varies irregularly with sampling depth (Fig. 7). The most primitive samples have MgO contents >10 wt%, Mg# up to 0.74 (Mg#= molar MgO/MgO+FeOt), Ni up to 300 ppm, Cr up to 800 ppm. They are comparable to and even more primitive than Kroenke lavas from the Ontong Java Plateau. Our new samples have TiO_2 =0.81-1.49 wt% and Al_2O_3/TiO_2 =10.4-17.1, except the petrographically distinct *Hbl*-gabbro ROV3-4 (TiO_2 = 2.03 wt%; Al_2O_3/TiO_2 = 9) and very fine-grained sample ROV3-11 (TiO_2 = 0.72 wt%; Al_2O_3/TiO_2 =20) (Fig. 3) and are compositionally similar to the previously reported high-Ti series of Manihiki lavas from DSDP Site 317A and dredge locations at the northwestern tip of the High Plateau (Hoernle et al., 2010; Timm et al., 2011) (Fig. 6). The ROV samples, however, seem to have slightly elevated SiO_2 and lowered FeO at similar MgO content. Relatively high TiO_2 (>0.5 wt.%) and P_2O_5 and low Sc distinguishes the high-Ti samples from the low-Ti series of Manihiki rocks, which otherwise have similar major element compositions. The compositions are also similar to OJP lavas, particularly to the dominant Kwambaita group in terms of TiO_2 content, but have ~2 wt% higher SiO_2 and partly overlapping and lower FeO_t and CaO contents (Fig. 6). Sample ROV3-11 has low TiO_2 (0.74 wt%) similar to Kroenke lavas. Elevated Na_2O content in some ROV samples can be related to albitization of plagioclase and shows a crude, nonetheless significant (r^2=0.43, n=19), positive correlation with SiO_2.

The major element systematics of Manihiki and OJP lavas is consistent with crystallization of a simple basaltic assemblage of minerals from primitive high-MgO parental magma. The mineral assemblage comprises olivine, which was joined by plagioclase at ~ 9 wt% MgO and by clinopyroxene at ~8 wt% MgO as is testified by modelling in Petrolog3 software (Danyushevsky and Plechov, 2011) (Fig. 6) and in agreement with petrographic observations (Table 2; Fig. 3).

The *Hbl*-gabbro has the most evolved composition. It also has distinctively higher Al_2O_3, TiO_2 and Na_2O but lower CaO and FeO (Fig. 6). Greenschist sample ROV4-14 has elevated SiO_2, low CaO and elevated Na and Sc contents but incompatible trace element and isotope compositions similar to the majority of the ROV samples. The distinctive major element composition of this sample likely reflects pervasive albitization of plagioclase and Ca loss during metamorphism.

4.2.3. Incompatible trace elements

Concentrations of incompatible trace elements in samples recovered by ROV fall within a relatively narrow range (Fig. 7, 8). Concentrations of moderately incompatible elements such as heavy REE (HREE) and Y correlate negatively with MgO in agreement with expected effects of fractional crystallization. Incompatible element concentrations normalized to primitive mantle composition have a slightly convex-up shape with nearly constant $(Dy/Yb)_N$=1.20-1.24 and variable light to middle REE ratios, e.g. $(La/Sm)_N$=0.7-1.1. The multi-element patterns have shapes similar to those of the previously reported high-Ti Manihiki samples such as from DSDP Site 317A (Fig. 8; Hoernle et al., 2010). The compositions exhibit crude trends of depletion in ratios of moderately incompatible relative to less incompatible elements (e.g., decreasing Zr/Y, La/Sm) with decreasing sampling depth (Fig. 7). Previously reported composition of sample SO193-DR46-1 dredged from the summit area of the tectonic block plots on the extension of the ROV trend toward shallower depths.

The ROV samples exhibit a continuous range of compositions but for convenience can be subdivided into two groups with different enrichment/depletion in LREE. Most samples from the lower part of the ROV profile (metadolerites) and two rocks from the upper part (*Pl*-*Px* phyric lavas) have nearly flat light to middle REE trace element patterns with $(La/Sm)_N$=0.92-1.11. These lavas are akin to the lowermost lava units in DSDP Site 317A and have incompatible-element compositions broadly intermediate between the Kwambaita and Singgalo lavas (Tejada et al., 2002; Fitton, Godard, 2004). The absolute HREE concentrations in all but one ROV sample are lower than in the DSDP Site 317A samples, reflecting more primitive composition of the ROV samples, and correlate inversely with MgO (Fig. 8). Rocks from the upper part of the ROV profile tend to have more convex-up spectra with $(La/Sm)_N$=0.7-0.85. They have similar multi-element patterns to those from the uppermost units of the DSDP Site 317A and Kwambaita lavas.

Composition of very fine-grained basalt ROV3-11 is different from other samples, having low "MORB-like" $(Dy/Yb)_N$=0.94 and low $(Ce/Yb)_N$=0.53. The sample has more fractionated incompatible-element spectra than all high-Ti Manihiki samples and OJP lavas, but not as depleted in HREE as low-Ti Manihiki rocks (Golowin et al., 2017a, b). The sample has transitional composition between high- and low-Ti samples and in this respect has no analogues among previously published data from Manihiki Plateau. Greenschist sample ROV4-14 has trace element pattern similar to rocks from the LREE depleted ($(La/Sm)_N<0.9$) group. The sample has minor Ce depletion relative to La and Nd, not typical for other ROV samples but common in Manihiki lavas and is likely related to postmagmatic processes. The *Hbl*-gabbro has a distinctive spectra compared to other ROV samples, as well the highest $(Dy/Yb)_N$=1.43 and $(Ce/Yb)_N$=2.1. The sample also exhibits a prominent enrichment in Ti, Nb and depletion in Th.

Samples of highly altered lavas have $(Dy/Yb)_N$=1.2-1.4 and $(Ce/Yb)_N$=1.1-1.3, which are similar to other high-Ti rocks of low-La/Sm group. The lava samples, however, have much higher $(La/Sm)_N$ =1.3-1.7 and exhibit strong negative Ce anomalies. The REE systematics can be best explained by uptake of LREE during low-*T* alteration of these rocks at oxidizing conditions, when trivalent REEs are more mobile than Ce^{4+} (e.g., Le Roex et al., 2010 and ref. therein).

The concentrations of Nb (and Ta) in high-Ti Manihiki samples are variable and range from higher to lower mantle-normalized values relative to similarly incompatible La and Th. The behaviour of Nb can be evaluated using the parameter $Nb/Nb^* = Nb_N/(Th_N{*}La_N)^{0.5}$, which quantifies the magnitude of Nb depletion (Nb/Nb*<1) or enrichment (Nb/Nb*>1) relative to Th and La. Nb/Nb* in Manihiki samples ranges from 0.8 to 1.3 and correlates inversely with $(La/Sm)_N$ and $(Ce/Yb)_N$ (Fig. 9). The most LREE depleted ROV samples approach the compositions of the most LREE depleted low-Ti rocks, which have high Nb/Nb* = 1.4-1.7 and highly variable $(Ce/Yb)_N$ =0.2-2.0 due to variable contribution of Nb-rich HIMU-like component to highly depleted mantle (Golowin et al., 2017a). In comparison with the high-Ti Manihiki series, OJP lavas exhibit a similar negative correlation between Nb/Nb* and LREE enrichment but they have higher Nb/Nb* at $(Ce/Yb)_N$ similar with Manihiki rocks, so that even the most LREE-rich Singgalo rocks do not have a negative Nb anomaly (Nb/Nb*<1).

Concentrations of highly mobile alkali elements (K, Rb) are disturbed in the rocks due to metamorphism and do not correlate with immobile elements. Less mobile alkali earth elements (Sr, Ba), Pb and U exhibit less variability, and their ratios are close to the 'canonical' ratios for oceanic basalts in most samples. For example, Ce/Pb=26±8 (1σ) and Nb/U=36±9 (1σ) in the ROV samples are close to typical Ce/Pb = 25±5 and Nb/U = 47±10 in oceanic basalts (Hofmann et al., 1986). Slightly low Nb/U in the ROV samples, as well as in DSDP Site 317A basalts (Nb/U =36±7, 1σ; Hoernle et al., 2010), is a characteristic feature of EM1 basalts (Hofmann, 1997).

4.2.4. Sr-Nd-Pb isotopes

All isotope ratios were corrected for ingrowth of daughter isotope assuming the age of 120 Ma and using element concentrations measured by ICP-MS. Most of the high-Ti ROV samples have nearly uniform unradiogenic εNd(t) = 1.8-2.2 and partly overlap with previously reported compositions of high-Ti lavas from the lower units of the DSDP Site 317A and dredged samples. The most depleted N-MORB-like sample ROV3-11 has higher εNd (t) = 3.6 similar to the εNd(t) in the uppermost units of the DSDP Site 317A. $^{87}Sr/^{86}Sr$ (t) are scattered consistent with variable addition of seawater Sr. The lowest $^{87}Sr/^{86}Sr$ (t) are similar to those previously reported from relatively fresh high-Ti Manihiki lavas (Hoernle et al., 2010; Timm et al., 2011). The ROV samples have relatively low U concentrations, and thus correction for the radiogenic ingrowth ^{206}Pb and ^{207}Pb isotopes is small. The age corrected Pb isotope ratios fall within a narrow range and form positive correlations on the uranogenic and thorogenic isotope diagrams. Pb isotope ratios become less radiogenic with decreasing sampling depth (Fig. 7). Sample SO193-DR46-1 from the shallowest portion of the sampled structure has Pb isotope ratios plotting on this trend. εNd(t) is nearly uniform throughout the ROV profile.

Overall, the high-Ti rocks have compositions trending towards the EM1 mantle end member having low εNd and $^{206}Pb/^{204}Pb$, elevated Δ7/4 and Δ8/4 and high $^{87}Sr/^{86}Sr$ (Zindler and Hart, 1986; Hofmann, 1997). Compared to Singgalo group lavas, which also have EM1-like isotopic compositions (Tejada et al., 2002; 2004), the high-Ti Manihiki lavas have lower εNd(t). In comparison with all OJP rocks, high Ti-Manihiki lavas have lower εNd(t), except *Hbl*-gabbro sample ROV3-4. Both high-Ti Manihiki and the three groups of OJP rocks (Kroenke, Kwaimbaita and Singgalo) have distinctively higher Δ8/4 and lower εNd(t) compared to Cretaceous Pacific MORB (Fig. 10).

The *Hbl*-gabbro sample ROV3-4 has distinct Sr-Nd-Pb isotopic composition compared to the other high-Ti samples. This sample has a similar isotopic composition to Kroenke/Kwaimbaita lavas but with slightly higher $^{207}Pb/^{204}Pb$ and $^{208}Pb/^{204}Pb$ isotope ratios.

5. Discussion

5.1 Composition of primary high-Ti magmas and potential mantle temperature

A new result from this study is the identification of very primitive high-Ti rocks with Mg# up to 0.73, approaching primary mantle melt compositions (e.g., Herzberg, 2011). In this respect the ROV samples are similar to Kroenke-type OJP lavas (Fitton and Godard, 2004), permitting direct comparison of these rock series.

Primary olivine phenocrysts were not preserved in the Manihiki rocks and thus direct assessment of the liquidus olivine composition was not possible. In order to calculate the composition of primary mantle melts and their potential mantle temperature (T_p), we used the MEGA PRIMELT3 Excel spreadsheet (Herzberg, Asimow, 2015), which is the latest version of the PRIMELT algorithm (Herzberg, Asimow, 2008). For primary magma calculation, we selected the most primitive high-Ti rock compositions with MgO>9 wt% from this study and also the most primitive rock compositions from the DSDP Site 317A. The calculations were performed assuming an accumulated fractional melting model. For the sake of comparison, T_p for primitive low-Ti Manihiki rock compositions (Golowin et al., 2007b), Kroenke-type lavas (Fitton and Godard, 2004) and also rocks from other large igneous provinces from the compilation of Herzberg and Gazel (2009) were recalculated using the same approach. This was required because the newest PRIMELT3 software returns 10 to 20 ^{o}C lower T_p compared to PRIMELT2 (Herzberg, Asimow, 2015). More importantly, our calculation was performed for accumulated fractional melting for all settings, whereas batch and accumulated fractional melting models were used in previous studies hampering comparison of the data. For example, all results reported by Herzberg and Gazel (2009) were obtained using batch melting model, and thus all *Tp* are up to 60 ^{o}C higher compared to the estimates for the same rocks using fractional melting model. T_p for the Kroenke-type OJP magmas have been estimated to be on average 1540 ^{o}C by Herzberg and Gazel (2009) and 1480 ^{o}C using fractional melting model in the latest version of PRIMELT (Herzberg et al., 2007; Herzberg, Asimow, 2015). The estimated uncertainty of T_p estimates with PRIMELT3 used in this study is 38.5 ^{o}C

(Herzberg, Asimow, 2015). The results of our calculations and updated dataset for large igneous provinces are presented in Fig. 11 and Supplementary table 4.

The estimated T_p for high-Ti Manihiki series are scattered from 1323 to 1516 °C due to the variability in bulk rock Fe content (Fig. 6), likely related to post-magmatic processes. The majority of the estimates, however, cluster near T_p~1450°C and correspond to primary magmas with 16 wt% MgO resulting from 27-30% peridotite melting starting at ~3 GPa and ending at ~1.0 GPa (Herzberg at al., 2007). The T_p estimates extend to higher temperatures compared to the low-Ti Manihiki series with median T_p= 1432°C.

The average T_p estimates for the Kroenke magmas are higher (c. 1480 °C) than the averages for Manihiki high- and low-Ti lavas, but overlap the range of the high-Ti Manihiki rocks. In comparison with other large igneous provinces, the PRIMMELT3 estimates for the Manihiki magmas suggest a relatively low T_p, only exceeding those for the Central Atlantic magmatic Province and comparable with OJP and Siberian Traps. T_p estimates in excess of 1500 °C were obtained for some samples from Deccan Traps, Caribbean Large Igneous Province and Greenland.

Golowin et al. (2017a,b) argued that low-Ti Manihiki magmas result from two-stage melting of mantle peridotite. This can also affect the T_p estimates made with the help of the PRIMELT3 software. A modelling of two-stage peridotite melting is currently not possible with this software. However, the effects of previous mantle depletion on the T_p estimate can be assessed by changing the initial MgO content in mantle peridotite, which increases with increasing depletion of mantle peridotite in basaltic component (e.g., Maaloe, Aoki, 1977; Baker, Beckett, 1999; Herzberg, 2004b). The initial source composition is pre-set to 38.12 wt% MgO in PRIMELT3 that is close to MgO in primitive mantle (37.8-38.8 wt%; McDonough, Sun, 1995). Assuming that the source of low-Ti Manihiki magmas is more depleted than primitive mantle and contains 41.5 wt% MgO after first-stage 10% melting at 1-3 GPa pressure (Herzberg et al., 2009), the calculated T_p increases by 40 °C and becomes very similar to OJP basalts (~1480 °C; Fig. 11). Melting of the refractory mantle should start at ~3 GPa, shallower than for OJP but at similar pressure to the high-Ti Manihiki magma source, and could produce ~15-20% melt during decompression to 1 GPa (Herzberg at al., 2007), about 2 times less melt compared to melting of similarly hot but more fertile source of OJP and high-Ti Manihiki magmas.

Compared to the T_p inferred for the upper mantle source for MORB (1300-1400 °C; Herzberg et al., 2007), T_p of Manihiki mantle sources are at least 30-50 °C higher (Fig. 11) and thus are compatible with the plume-related origin of this plateau, which is favoured in most previous publications.

5.2 Compositional heterogeneity and temporal trends of the high-Ti rock series

The new data show that high-Ti basalts represent an important rock type of the Manihiki basement. They are likely to be at least as common as the low-Ti rocks, which were extensively sampled along the Danger Island and Suvorov Troughs and prevail in the published datasets (Ingle et al. 2007; Timm et al., 2011; Golowin et al., 2017a,b). A limited major element variability of the least altered high-Ti rocks suggests that their compositions were mostly governed by fractional crystallization from a parental melt with a narrow compositional range (Fig. 6). Incompatible elements and isotope ratios in high-Ti rocks are more variable (Fig. 7-9) and cannot be explained by magma crystallization processes. They imply the presence of subordinate, compared to the mantle peridotite, and compositionally variable enriched components in the mantle source or variably enriched peridotite sources. The new data together with previously published results (Hoernle et al., 2010; Timm et al., 2011) allows us to refine the existing systematics of the high-Ti rocks and to define distinct compositional groups based on their Nd isotope ratios (Fig. 10).

One group includes the majority of “normal-type” ROV samples and previously reported high-Ti lavas from the northern edge of the Central Plateau (Timm et al., 2011), except sample SO193-DR49-1 dredged from a seamount at the northwestern tip of the Central Plateau. The rocks show correlated variations in Pb isotope ratios ($^{206}Pb/^{204}Pb$ = 17.84-18.24, $^{207}Pb/^{204}Pb$ =15.49-15.53, and $^{208}Pb/^{204}Pb$ =38.06-38.37; Fig. 10 c, d) and a narrow range in εNd(t)= 1.8-2.3. Correlation between the thorogenic and uranogenic ratios precludes the origin of the Pb isotope heterogeneity due to under- or overcorrection for the radiogenic Pb ingrowth (e.g., Hauff et al., 2003). Dredged lava samples have the least radiogenic Pb isotope ratios in this group and are also the most depleted in highly incompatible elements (Ce_N/Yb_N<0.9). This observation and also a decrease in $^{206}Pb/^{204}Pb$, Zr/Y and La/Sm ratio in ROV samples with decreasing sampling depth (Fig. 7) suggest temporal evolution from more to less radiogenic Pb isotope compositions associated with melt depletion in incompatible elements. Interestingly, some samples from this group are depleted in LREE and have Nb/Nb*>1, particularly the most REE depleted sample SO225-ROV3-11 with Nb/Nb*=1.3, Nb_N/Ce_N =1.1 and Ce_N/Yb_N=0.52. The trace element pattern cannot be generated by partial mantle melting alone (e.g., Stracke and Bourdon, 2009), implying the presence of Nb-rich component with higher εNd than in low Nb/Nb* component but with an EM1 type Pb isotope composition.

The lavas with the least radiogenic Pb isotope compositions have ages 125-127 Ma, some of the oldest reported for the Manihiki plateau (Timm et al., 2011). The stratigraphically lower ROV samples presumably have older ages and indicate P-T conditions of middle to lower crust (Fig. 3). Therefore we propose that the group 1 high-Ti rocks characterize a relatively early (perhaps, the main) stage of the plateau formation. The coupled variations of Pb isotopes and trace elements cannot be explained by variable degrees of melting of homogeneous mantle source (e.g., Stracke and Bourdon, 2009) and imply involvement of at least two different mantle components with similar Nd and Sr but different Pb isotope and possibly incompatible-element composition during this stage of the plateau formation.

The second group of high-Ti rocks is represented by basalts from DSDP Site 317A (Fig. 8). These rocks were dated at 116-117 Ma (Hoernle et al., 2010) and thus are 9-10 Ma younger compared to the first group. These rocks have distinctively lower ^{207}Pb/^{204}Pb (15.46-15.48) and overall lower ^{208}Pb/^{204}Pb (38.06 - 38.28) but higher εNd (2.4 - 3.8) compared to the first group. Pb isotope ratios and εNd correlate in this group so that the compositions become more radiogenic and more depleted in incompatible elements with decreasing core depth. The correlation between ^{206}Pb/^{204}Pb and ^{207}Pb/^{204}Pb is steeper than in the first group and can be extrapolated to the composition of amphibole gabbro SO225-ROV3-4 with the most radiogenic Pb and Nd of all samples studied, as is also the case with most of the ROV samples. Tentatively we include in the second group sample SO193-DR49-1 reported by Timm et al. (2011), which was dredged from a seamount (Werner and Hauff, 2007). This sample has elevated εNd and low ^{207}Pb/^{204}Pb, unlike the first group samples (Fig. 10). Due to their younger age, we propose that the second group of rocks represent the final stages of the Manihiki plateau formation and perhaps transition to the late-stage alkalic volcanism, which occurred after the main stage of plateau formation (e.g., Ingle et al., 2007; Hochmuth et al., 2015; Beiersdorf et al., 1995).

5.3 The origin of source components in Manihiki magmas

Despite some heterogeneity, the enriched component in high-Ti Manihiki magmas has EM1-type trace element and isotopic composition (Zindler, Hart, 1988; Eisele et al., 2002; Willbold and Stracke, 2006). Specific features of this component include low Nb/Nb*, low εNd, low ^{206}Pb/^{204}Pb but high ^{208}Pb/^{204}Pb (Fig. 10). An EM1-type component is also present on the OJP and represented by the Singgalo lavas (Tejada et al., 2002). The enriched EM1 component in the high-Ti rocks, however, differs from the Singgalo-type EM1, due to its different isotopic composition (Fig. 10) and lower Nb/Nb* (Fig. 9).

The origin of EM1 component in oceanic magmas has been discussed in detail in many publications (Woodhead and Mcculloch, 1989; Lassiter, Hauri, 1998; Eisele et al., 2002; Tanaka et al., 2008; Stracke et al., 2004; Willbold, Stracke, 2004; Geldmacher et al. 2008; Collerson et al., 2010; Turner et al., 2017). Presently the prevailing view on the origin of EM1 component relates its peculiar geochemical features to recycling of lower continental crust either via subduction or by delamination of the continental lithosphere (e.g., Chauvel et al., 1992; Eisele et al., 2002; Willbold and Stracke, 2006; 2010; Tejada et al., 2013). Alternative hypotheses include involvement of subcontinental lithospheric mantle (e.g., Cohen, O'Nions, 1982; Hawkesworth et al., 1990; Geldmacher et al., 2008; Hoernle et al., 2010) and mantle metasomatism by CO_2-rich melts under lower mantle conditions (Collerson et al., 2010).

Trace element and isotope compositions of the high-Ti Manihiki rocks reported in this study are consistent with a possible origin of the EM1 component by recycling of lower continental crustal material. Particularly informative is the low Nb/Nb* in these rocks, which indicates the involvement of Nb depleted continental crustal material (Eisele et al., 2002). Willbold and Stracke (2006) suggested a number of additional trace element indicators of recycled continental crustal components in the sources of oceanic basalts. Eu/Eu* ratio in the high-Ti Manihiki rocks is scattered from 0.8 to 1.1 (on average 1.0) and thus does not provide conclusive evidence about the origin of continental crustal components. Most other indicators proposed by Willbold and Stracke (2006) use alkalis and alkali earth elements and cannot be applied with confidence to the altered and metamorphosed rocks studied here. However, new LA-ICP-MS data for pristine glass from sample SO193-DR52-1 (Supplementary Table 1) yields Ba/Nb=12, Rb/Nb=0.94, Th/Rb=0.12, Ba/Rb=12.6, Eu/Eu*=0.97 consistent with ≤ 1 wt% lower continental crust material in the source of the high-Ti rocks (Willbold and Stracke, 2006).

Tejada et al. (2013) argued that the lower crustal component in the source of Singgalo rocks is the most similar to Archean mafic granulites such as the Lewisian gneises from northwestern Scotland (Weaver, Tarney, 1980). Characteristic geochemical features of these crustal rocks include moderate enrichment in LREE (Ce_N/Yb_N= 1.8-2.8), Th depletion relative to La and Ta (Nb) (Th_N/Ta_N =0.18-0.57, Th_N/La_N=0.1-0.6) and no systematic Nb-Ta depletion relative to La (Ta_N/La_N =0.47-1.20). Unlike the Archean gneises and Singgalo rocks, high-Ti Manihiki basalts show coupled depletion in Nb and Th relative to La and less fractionated Th_N/Ta_N ≈0.8 and Th_N/Nb_N≈1 (Fig. 8). This suggests that the enriched component in the source of high-Ti magmas had a different composition. The majority of high-Ti rocks have low Nb/Nb* (Fig. 9) and thus, unlike the Singgalo rocks, their compositions are more consistent with the involvement of Nb-depleted lower crustal material (e.g., Rudnick and Gao, 2003) mixed with undepleted mantle peridotite.

Alternatively, Hoernle et al. (2010) and Timm et al. (2011) proposed that high-Ti Manihiki magmas might originate from recycled subcontinental lithospheric mantle (SCLM). Sr-Nd-Pb isotope composition of SCLM agree well with end member EM1 composition (e.g., Cohen, O'Nions, 1982; Hawkesworth et al., 1990; Geldmacher et al., 2008). Recently, Schaefer et al. (2015) reported $^{187}Os/^{188}Os(t)$ in primitive Manihiki rocks ranging from 0.17 to as low as 0.106. The lowest values are significantly lower than Phanerozoic primitive mantle (chondrite) values of 0.125-0.130 (Meisel et al., 1996; Shirey and Walker, 1998), and suggest involvement of Archean depleted mantle with low time-integrated Re/Os (e.g., Carlson and Irving, 1994; Reisberg, Lorand, 1995). In contrast to these results, Tejada et al. (2013) reported near-chondritic $^{187}Os/^{188}Os(t) \approx 0.13$ in Kroenke- and Kwambaita rocks, suggesting a primitive mantle source. Singgalo EM1-type rocks were found to have super-chondritic $^{187}Os/^{188}Os(t) = 0.330 \pm 0.018$, suggesting involvement of an ancient, possibly delaminated mafic continental crust. The low Os concentrations (10-37 ppt) of the Singgalo samples, however, made the lavas prone to crustal contamination during plateau emplacement, which could potentially explain the high Os isotope ratios. Low $^{187}Os/^{188}Os(t)$ in Manihiki rocks, on the other hand, contrast with superchondritic $^{187}Os/^{188}Os(t)$ reported for EM1-type rocks from

Koolau, Hawaii (up to 0.148; Lassiter and Hauri, 1998) and Pitcairn Archipelago (up to 0.15; Eisele et al., 2002), which also suggest involvement of recycled crustal material in the formation of the EMI compositions of these rocks (Saal et al., 1998; Peucker-Ehrenbrink and Borming, 2001).

The presently available incompatible element and Sr-Nd-Pb isotope data are generally consistent with both alternative models, suggesting the origin of high-Ti basalts either from a mixture of lower continental crust with undepleted (fertile) mantle, similarly with Singgalo type OJP lavas (Tejada et al., 2013) or from recycled and re-fertilized subcontinental lithospheric mantle (Hoernle et al., 2010; Timm et al., 2011). In any case, both alternatives require the involvement of continental lithosphere, even if we cannot distinguish whether lower crust and/or subcontinental lithospheric mantle were involved. Publication of the Re/Os results from Manihiki can help to distinguish between these possibilities.

5.4. Are OJP and Manihiki parts of one single plateau?

The Ontong Java, Manihiki and Hikurangi Plateaus are widely believed to represent disintegrated parts of a single Ontong Java Nui "super"-plateau, making it the biggest one in the Phanerozoic (e.g., Taylor, 2006; Davy et al., 2008; Chandler et al., 2012; Hochmuth et al., 2015). Our new data on the composition of a deeper portion of the Manihiki crust, as well as recent data on geochemistry of low-Ti Manihiki rock series (Golowin et al., 2017a,b), significantly extend the available geochemical database and permit re-evaluation of possible genetic links between OJP and Manihiki.

Taking the new data into consideration, we have to conclude that presently sampled parts of OJP and Manihiki Plateaus are geochemically distinct. The compositions of different geochemical groups identified in both plateaus are not complimentary to each other and are distinguished in major elements (Fig. 6), trace elements (Fig. 8, 9) and isotope ratios (Fig. 9, 10). Unlike OJP, the Manihiki magmas are compositionally more diverse and do not exhibit clear temporal variations in geochemistry. At OJP, early volcanism tapped a more depleted (Kroenke and Kwambaita) source; more enriched (Singgalo) compositions were not erupted until the very end of plateau formation, as is evident from Singgalo lavas stratigraphically overlaying Kwaimbaita lavas in drilled and subaerial outcrops.

A particularly distinctive feature of the Manihiki Plateau is the presence of low-Ti rocks, which originated from melting of highly refractory source (Ingle et al., 2007; Golowin et al., 2007a,b). In contrast, a major source of OJP basalts was an undepleted near-primitive mantle (Tejada et al., 2004; Fitton and Godard, 2004; Jackson and Carlson, 2011). At similar T_p and final depths of melting, the on average more depleted source under Manihiki would have been less productive and generated thinner crust in comparison to melting of fertile mantle under OJP (Tejada et al., 2004; Fitton and Gordon, 2004) (see also section 5.1). Melting of a more depleted source under Manihiki, therefore, could explain the lower crustal thickness under the Manihiki Plateau (c. 20 km) compared to OJP (>30 km) (Furumoto et al., 1976; Coffin, Eldholm, 1994; Hochmuth et al., 2015), which is not accounted for by previously suggested models of similar parental mantle composition for both plateaus.

Despite the compositional differences, OJP and Manihiki Plateaus were formed nearly contemporaneously within the precision of the available age data (e.g. Timm et al., 2011) and spatially close to each other (e.g. Taylor, 2006; Davy et al., 2008; Chandler et al., 2012). The mantle sources of these plateaus had similar mantle potential temperatures (e.g., Timm et al., 2011; Golowin et al., 2017a; this study) (Fig. 11). It is thus possible that they were formed by melting of a single but compositionally heterogeneous mantle plume. The geochemical data cannot distinguish whether OJP and Manihiki Plateau originally formed a single plateau (e.g. Taylor, 2006; Davy et al., 2008) that tectonically separated along the boundary between compositionally different geochemical domains, for example, due to different crustal thickness. Alternatively, they could have formed from two separate branches of a single deep-rooted plume, which could have split at depth due to compositional differences and thus rheological properties and formed closely spaced but separate igneous plateaus (e.g. Larson, 1997).

6. Conclusions

- A profile along the southeastern margin of a seamount between the Manihiki Northern and Western plateaus was sampled between water depths of 4600 and 3300 m.b.s.l. with the remotely operated vehicle (ROV) Kiel 6000 during R/V Sonne SO225 expedition. The profile represents a section of deep igneous crust, metamorphosed under greenschist to amphibolite facies.
- The rocks belong to high-Ti Manihiki series and have an age ≥125 Ma, as they have stratigraphically lower position relative to a previously dated sample from the top of the seamount. The samples are the most primitive high-Ti basalts recovered from the Manihiki Plateau and allow us to assess the composition of primary melts and their geochemical variability. A single sample of hornblende gabbro was also recovered, possibly derived from an intrusion related to the late-stage alkalic volcanism following the main stage of plateau formation.
- Estimated mantle potential temperatures for Manihiki rocks are comparable to those for Ontong Java Plateau (1450-1480 ^{o}C) but are not as high as inferred for some other large igneous provinces (>1500 ^{o}C). The temperatures are high compared to the upper mantle and suggest a lower mantle plume source. An updated and consistent dataset for mantle temperatures of large igneous provinces is presented.
- High-Ti Manihiki rocks exhibit strong EM1 type Sr-Nd-Pb isotopic signature, which can be explained either by melting of a mixture of recycled lower continental crust and fertile mantle or by melting of recycled re-fertilized subcontinental lithospheric mantle.
- A distinctive feature of the Manihiki Plateau mantle source is the presence of highly depleted and variably re-fertilized mantle peridotite, which was a primary source of low-Ti

magmas and could also contribute to the origin of high-Ti magmas. On average more depleted and therefore less productive mantle source can explain the lower crustal thickness of the Manihiki plateau compared to OJP, which was formed by melting of a more fertile mantle with similar potential temperature.

- The presently available geochemical data for Manihiki and Ontong Java Plateaus shows that the compositions of rocks constituting these large igneous provinces in the Western Pacific, as well as their mantle sources, were different. Therefore, the mantle sources of these plateaus either formed 1) two large but separated domains within a single plume or 2) two compositionally and spatially different but temporally closely associated plumes rising from the lower mantle, or a single upwelling that split before reaching conditions of partial melting.

7. Acknowledgements

We thank Captain Mallon, the crew and the scientific participants of the SO225 cruise, especially the technical/scientific ROV-crew, for excellent collaboration. Further, we are grateful to U. Westernströer, K. Junge and S. Hauff for assistance with sample preparation and supervision of ICP-MS and TIMS analyses. We thank Michael Bizimis, Maria Luisa Tejada and Stephen Turner for their detailed and constructive reviews, which helped significantly improve this manuscript and Catherine Chauvel for editorial handling of this manuscript. This study was funded as part of the MANIHIKI II project by the German Ministry of Education and Research (BMBF, Manihiki II project; #03G0225A).

8. References

Abouchami W, Galer SJG, Hofmann AW (2000) High precision lead isotope systematics of lavas from the Hawaiian Scientific Drilling Project. Chemical Geology 169:187–209

Beiersdorf H, Bach W, Duncan R, Erzinger J, Weiss W (1995) New evidence for the production of EM-type ocean island basalts and large volumes of volcaniclastites during the early history of the Manihiki Plateau. Marine Geology 122: 181-205.

Baksi, A.K., 2007. A quantitative tool for detecting alteration in undisturbed rocks and minerals – I: Water, chemical weathering and atmospheric argon. In: Foulger, G.R., & Jurdy, D.M. (Eds.) The Origin of Melting Anomalies, Plates, Plumes and Planetary Processes. Geological Society of America, Special Papers, 430, 285-303.

Baker MB, Beckett JR (1999) The origin of abyssal peridotites: a reinterpretation of constraints based on primary bulk compositions. Earth Planet Sci Lett 171:49-61

Billen, M. I., and J. Stock (2000), Morphology and origin of the Osbourn Trough, J. Geophys. Res., 105(B6), 13,481–13,489, doi:10.1029/2000JB900035.

Carlson RW, Irving AJ (1994) Depletion and enrichment history of subcontinental lithospheric mantle: An Os, Sr, Nd and Pb isotopic study of ultramafic xenoliths from the northwestern Wyoming Craton. Earth Planet Sci Lett 126(4):457-472 doi: 10.1016/0012-821X(94)90124-4

Castillo PR, Klein E, bender J, Langmuir C, Shirey S, Batiza R, White W (2000) Petrology and Sr, Nd, and Pb isotope geochemistry of mid-ocean ridge basalt glasses from the 11o45'N to 15o00'N segment of the East Pacific Rise. Geochem Geophys Geosyst 1(11), 1011, doi: 10.1029/1999GC000024.

Chauvel C, Hofmann AW, Vidal P (1992) HIMU-EM, the French Polynesian connection. Earth Planet Sci Lett 110:99-119

Chandler, M.T. et al., 2012. Reconstructing Ontong Java Nui: Implications for Pacific absolute plate motion, hotspot drift and true polar wander. Earth and Planetary Science Letters, 331: 140-151.

Clague, D.A., et al., 1976. Petrology of basaltic and gabbroic rocks dredged from the Danger Island Troughs, Manihiki Plateau. In: Schlanger, S.O., Jackson, E.D. (Eds.), Initial Reports of the Deep Sea Drilling Project, Volume 33. U.S. Government Printing Office, Washington, D.C., pp. 891–907.

Coffin, M.F., Eldholm, O., 1994. Large Igneous Provinces - Crustal Structure, Dimensions, and External Consequences. Reviews of Geophysics, 32(1): 1-36.

Cohen RS, O'Nions R, K. (1982) Identification of recycled continental material in the mantle from Sr, Nd and Pb isotope investigations. Earth Planet Sci Lett 61:73-84

Collerson KD, Williams Q, Ewart AE, Murphy DT (2010) Origin of HIMU and EM1 domains sampled by ocean island basalts, kimberlites and carbonatites: The role of CO2-fluxed lower mantle melting in thermochemical upwellings. PEPI 181(3):112-131 doi: 10.1016/j.pepi.2010.05.008

Danyushevsky, L.V., Plechov, P., 2011. Petrolog3: Integrated software for modeling crystallization processes. Geochemistry Geophysics Geosystems, 12(7).

Davy, B., Hoernle, K., Werner, R., 2008. Hikurangi Plateau: Crustal structure, rifted formation, and Gondwana subduction history. Geochemistry Geophysics Geosystems, 9(7).

Eisele J, Sharma M, Galer SJG, Blichert-Toft J, Devey CW, Hofmann AW (2002) The role of sediment recycling in EM1 inferred from Os, Pb, Hf, Nd, Sr isotope and trace element systematics of the Pitcairn hotspot. Earth Planet Sci Lett 196(3–4):197-212 doi: 10.1016/S0012-821X(01)00601-X

Fitton, J.G., Godard, M., 2004. Origin and evolution of magmas on the Ontong Java Plateau. Fitton J. G., Mahoney, J. J., Wallace, P. J., Saunders, A. D. (eds), Origin and Evolution of the Ontong Java Plateau: Geological Society, London, Special Publications, 229, pp. 151-178.

Frisby, C., Bizimis, M., Mallick, S., 2016. Seawater-derived rare earth element addition to abyssal peridotites during serpentinization. Lithos, 248-251: 432-454

Fodor RV, Bauer GR, Jacobs RS, Bornhorst TJ (1987) Kahoolawe Island, Hawaii: tholeiitic, alkalic and unusual hydrothermal(?) "enrichment" characteristics. J Volcanol Geotherm Res 31:171-176

Furumoto, A. S., J. P. Webb, M. E. Odegard, and D. M. Hussong (1976), Seismic studies on the Ontong Java plateau, 1970, Tectonophysics, 34, 71–90, doi:10.1016/0040-1951(76)90177-3.

Geldmacher J, Hoernle K, Klugel A, van den Bogaard P, Bindeman I (2008) Geochemistry of a new enriched mantle type locality in the northern hemisphere: Implications for the origin of the EM1 source. Earth Planet Sci Lett 265(1-2):167-182

Golowin R, Portnyagin M, Hoernle K, Hauff F, Gurenko A, Garbe-Schönberg D, Werner R, Turner S (2017a) Boninite-like intraplate magmas from Manihiki Plateau require ultra-depleted and enriched source components. Nature Communications 8:14322 doi:10.1038/ncomms14322

Golowin R, Portnyagin M, Hoernle K, Sobolev A, Kuzmin D, Werner R (2017b) The role and conditions of second-stage mantle melting in the generation of low-Ti tholeiites and boninites: The case of the Manihiki Plateau and the Troodos Ophiolite. Contributions to Mineralogy and Petrology 172:104, DOI: 110.1007/s00410-00017-01424-00413

Hart SR, Staudigel H (1982) The control of alkalies and uranium in seawater by ocean crust alteration. Earth Planet Sci Lett 58:202-212

Hassler, D.R., Shimizu, N., 1998. Osmium isotopic evidence for ancient subcontinental lithospheric mantle beneath the Kerguelen Islands, southern Indian Ocean. Science, 280(5362): 418-421.

Hauff F, Hoernle K, Schmidt A (2003) Sr-Nd-Pb composition of Mesozoic Pacific oceanic crust (Site 1149 and 801, ODP Leg 185): Implications for alteration of ocean crust and the input into the Izu-Bonin-Mariana subduction system. Geochem Geophys Geosyst 4(8), 8913:doi:10.1029/2002GC000421

Hawkesworth, C.J., Erlank, A.J., Kempton, P.D., Waters, F.G., 1990. Mantle metasomatism: isotope and trace-element trends in xenoliths from Kimberley, South Africa. Chemical Geology, 85: 19-34.

Hawkesworth CJ, Kempton PD, Rogers NW, Ellam RM, van Calsteren PW (1990) Continental mantle lithosphere, and shallow level enrichment processes in the Earth's mantle. Earth Planet Sci Lett 96:256-268

Herzberg, C., 2004a. Partial melting below the Ontong Java Plateau. Fitton J. G., Mahoney, J. J., Wallace, P. J., Saunders, A. D. (eds), Origin and Evolution of the Ontong Java Plateau: Geological Society, London, Special Publications, 229, pp. 179-183.

Herzberg C (2004b) Geodynamic Information in Peridotite Petrology. J Petrology 45(12):2507-2530

Herzberg C, Asimow PD, Arndt N, Niu Y, Lesher CM, Fitton JG, Cheadle MJ, Saunders AD (2007) Temperatures in ambient mantle and plumes: Constraints from basalts, picrites, and komatiites. Geochem Geophys Geosyst 8, Q02006, doi:10.1029/2006GC001390

Herzberg C, Asimow PD (2008) Petrology of some oceanic island basalts: PRIMELT2.XLS software for primary magma calculation. Geochemistry Geophysics Geosystems 9 Artn Q09001, Doi 10.1029/2008gc002057

Herzberg, C., Gazel, E., 2009. Petrological evidence for secular cooling in mantle plumes. Nature, 458(7238): 619-22.

Herzberg C (2010) Identification of Source Lithology in the Hawaiian and Canary Islands: Implications for Origins. J Petrology 52(1):113-146 doi:10.1093/petrology/egq075

Herzberg C, Asimow PD (2015) PRIMELT3 MEGA.XLSM software for primary magma calculation: Peridotite primary magma MgO contents from the liquidus to the solidus. Geochemistry Geophysics Geosystems 16(2):563-578 doi:10.1002/2014GC005631

Hochmuth, K., Gohl, K., Uenzelmann-Neben, G., 2015. Playing jigsaw with Large Igneous Provinces-A plate tectonic reconstruction of Ontong Java Nui, West Pacific. Geochemistry, Geophysics, Geosystems: 1-19.

Hoernle, K. et al., 2010. Age and geochemistry of volcanic rocks from the Hikurangi and Manihiki oceanic Plateaus. Geochimica et Cosmochimica Acta, 74(24): 7196-7219.

Hofmann, A.W., Jochum, K.P., Seufert, M., White, W.M., 1986. Nb and Pb in oceanic basalts: new constraints on mantle evolution. Earth and Planetary Science Letters, 79(1/2): 33-45.

Hofmann, A.W., 1997. Mantle geochemistry: The message from oceanic volcanism. Nature, 385(6613): 219-229.

Holland T, Blundy J (1994) Nonideal Interactions in Calcic Amphiboles and Their Bearing on Amphibole-Plagioclase Thermometry. Contrib Mineral Petrol 116(4):433-447 doi: 10.1007/Bf00310910

Ingle, S., Coffin, M.F., 2004. Impact origin for the greater Ontong Java Plateau? Earth and Planetary Science Letters, 218(1-2): 123-134.

Ingle, S. et al., 2007. Depleted mantle wedge and sediment fingerprint in unusual basalts from the Manihiki Plateau, central Pacific Ocean. Geology, 35(7): 595-598.

Jackson, E.D., Bargar, K.E., Fabbi, B.P., Heropoulos, C., 1976. Petrology of the basaltic rocks drilled on Leg 33 of the Deep Sea Drilling Project. Initial Reports of the Deep Sea Drilling Project, 33: 571.

Jackson, M.G., Carlson, R.W., 2011. An ancient recipe for flood-basalt genesis. Nature, 476(7360): 316-9.

Korenaga, J., 2005. Why did not the Ontong Java Plateau form subaerially? Earth Planet. Sci. Lett. 234, 385–399.

Larson, R.L., 1991a. Geological consequences of superplumes. Geology 19 (10), 963–966.

Larson, R.L., 1991b. Latest pulse of Earth: evidence for a mid-Cretaceous superplume.Geology 19 (6), 547–555.

Larson, R.L., 1997, Superplumes and ridge interactions between Ontong Java and Manihiki Plateaus and the Nova-Canton Trough: Geology, v. 25, p. 779–782, doi: 10.1130/0091–7613(1997)025<0779:SARIBO>2.3.CO;2.

Lassiter JC, Hauri EH (1998) Osmium-isotope variations in Hawaiian lavas: evidence for recycled oceanic lithosphere in the Hawaiian plume. Earth Planet Sci Lett 164:483-496

le Roex A, Class C, O'Connor J, Jokat W (2010) Shona and Discovery Aseismic Ridge Systems, South Atlantic: Trace Element Evidence for Enriched Mantle Sources. J Petrol 51(10):2089-2120 doi:10.1093/petrology/egq050

Maaloe S, Aoki K (1977) The major element composition of the upper mantle estimated from the composition of lherzolites. Contrib Mineral Petrol 63:161-173

Mahoney, J.J., Spencer, K.J., 1991. Isotopic evidence for the origin of the Manihiki and Ontong Java oceanic plateaus. Earth and Planetary Science Letters, 104: 196-210.

Mahoney, J.J., Storey, M., Duncan, R.A., Spencer, K.J., Pringle, M., 1993. 1. Geochemistry and geochronology of Leg 130 basement lavas: Nature and origin of the Ontong Java Plateau. Proceedings of the Ocean Drilling Programm, Scientific results, 130.

Mahoney JJ, Sinton JM, Kurz MD, Macdougall JD, Spencer KJ, Lugmair GW (1994) Isotope and trace element characteristics of a super-fast spreading ridge: East Pacific rise, 13-23° S. Earth Planet Sci Lett 121(1-2):173-193

Masuda A, Nagasawa S (1975) Rocks with negative cerium anomalies, dredged from Shatsky Rise. Geochem J 9:227-233

Mcdonough, W.F., 1990. Constraints on the Composition of the Continental Lithospheric Mantle. Earth and Planetary Science Letters, 101(1): 1-18.

McDonough, W.F., Sun, S.S., 1995. The Composition of the Earth. Chemical Geology, 120(3-4): 223-253.

Meisel T, Walker RJ, Morgan JW (1996) The osmium isotopic composition of the Earth's primitive upper mantle. Nature 383:517 doi:10.1038/383517a0

Nakanishi M, Nakamura Y, Coffin MF, Hoernle K, Werner R (2015) Topographic expression of the Danger Islands Troughs and implications for the tectonic evolution of the Manihiki Plateau, western equatorial Pacific Ocean. GSA Special Papers, 511, p. SPE511-11, doi:10.1130/2015.2511(11).

Pearce JA, Norry MJ (1979) Petrogenetic implications of Ti, Zr, Y and Nb variations in volcanic rocks. Contrib Mineral Petrol 69:33-47

Peucker-Ehrenbrink B, Jahn B-m (2001) Rhenium-osmium isotope systematics and platinum group element concentrations: Loess and the upper continental crust. Geochemistry, Geophysics, Geosystems 2(10):n/a-n/a doi:10.1029/2001GC000172

Reisberg L, Lorand JP (1995) Longevity of Sub-Continental Mantle Lithosphere from Osmium Isotope Systematics in Orogenic Peridotite Massifs. Nature 376(6536):159-162

Regelous, M., Niu, Y., Wendt, J. I., Batiza, R., Greig, A., and Collerson, K.D., 1999, Variations in the geochemistry of magmatism on the East Pacific Rise at 10°30′N since 800 ka: Earth and Planetary Science Letters, v. 168, p. 45-63, doi:10.1016/S0012-821X(99)00048-5.

Rogers, G.C., 1982. Oceanic Plateaus as Meteorite Impact Signatures. Nature, 299(5881): 341-342.

Rudnick, R.L., Gao, S., 2003. Composition of the Continental Crust. In: Treatise on Geochemistry (Second Edition): 1-64.

Saal AE, Rudnick RL, Ravizza GE, Hart SR (1998) Re–Os isotope evidence for the composition, formation and age of the lower continental crust. Nature 393:58 doi:10.1038/29966

Schaefer BF, Hoernle K, Parkinson IJ, Golowin R, Portnyagin M, Turner S, Hauff F, Werner R (2015) Os isotope evidence for a heterogeneous source for the world's largest Phanerozoic volcanic event. Goldschmidt2015 Abstracts.

Shirey, S.B., Walker, R.J., 1998. The Re-Os isotope system in cosmochemistry and high-temperature geochemistry. Annual Review of Earth and Planetary Sciences, 26: 423-500.

Steiger, R.H., Jager, E., 1977. Subcommission on Geochronology - Convention on Use of Decay Constants in Geochronology and Cosmochronology. Earth and Planetary Science Letters, 36(3): 359-362.

Stracke, A., Bizimis, M., Salters, V.J.M., 2003. Recycling oceanic crust: Quantitative constraints. Geochemistry Geophysics Geosystems, 4(3): 1-33.

Stracke A, Bourdon B (2009) The importance of melt extraction for tracing mantle heterogeneity. Geochim Cosmochim Acta 73(1):218-238

Tanaka, R., Makishima, A., Nakamura, E., 2008. Hawaiian double volcanic chain triggered by an episodic involvement of recycled material: Constraints from temporal Sr–Nd–Hf–Pb isotopic trend of the Loa-type volcanoes. Earth and Planetary Science Letters, 265(3-4): 450-465.

Taylor, B., 2006. The single largest oceanic plateau: Ontong Java–Manihiki–Hikurangi. Earth and Planetary Science Letters, 241(3-4): 372-380.

Tejada, M.L.G., Mahoney, J.J., Duncan, R.A., Hawkins, M.P., 1996. Age and Geochemistry of Basement and Alkalic Rocks of Malaita and Santa Isabel, Solomon Islands, Southern Margin of Ontong Java Plateau. Journal of Petrology, 37(2).

Tejada, M.L.G., Mahoney, J.J., Neal, C.R., Duncan, R.A., Petterson, M.G., 2002. Basement Geochemistry and Geochronology of Central Malaita, Solomon Islands, with Implications for the Origin and Evolution of the Ontong Java Plateau. Journal of Petrology, 43(3).

Tejada, M.L.G. et al., 2004. Pin-pricking the elephant: evidence on the origin of the Ontong Java Plateau from Pb-Sr-Hf-Nd isotopic characteristics of ODP Leg 192 basalts. Fitton J. G., Mahoney, J. J., Wallace, P. J., Saunders, A. D. (eds), Origin and Evolution of the Ontong Java Plateau: Geological Society, London, Special Publications, 229, pp. 133-150.

Tejada, M.L.G. et al., 2013. Cryptic lower crustal signature in the source of the Ontong Java Plateau revealed by Os and Hf isotopes. Earth and Planetary Science Letters, 377-378: 84-96.

Tejada MLG, Geldmacher J, Hauff F, Heaton D, Koppers AAP, Garbe-Schonberg D, Hoernle K, Heydolph K, Sager WW (2016) Geochemistry and age of Shatsky, Hess, and Ojin Rise seamounts: Implications for a connection between the Shatsky and Hess Rises. Geochim Cosmochim Acta 185:302-327 doi:10.1016/j.gca.2016.04.006

Timm, C. et al., 2011. Age and geochemistry of the oceanic Manihiki Plateau, SW Pacific: New evidence for a plume origin. Earth and Planetary Science Letters, 304(1-2): 135-146.

Turner, S.J., et al., 2017, The importance of mantle wedge heterogeneity to subduction zone magmatism and the origin of EM1. Earth and Planetary Science Letters 472 (2017): 216-228.

Wendt JI, Regelous M, Niu Y, Hekinian R, Collerson KD (1999) Geochemistry of lavas from the Garrett Transform Fault: insights into mantle heterogeneity beneath the eastern Pacific. Earth Planet Sci Lett 173(3):271-284

Werner, R., Hauff, F., eds . 2007. FS Sonne, Fahrtbericht / Cruise Report SO193 MANIHIKI : Temporal, Spatial, and Tectonic Evolution of Oceanic Plateaus ; Suva/Fiji - Apia/Samoa, 19.05. - 30.06.2007 IFM-GEOMAR Report, 13 . IFM-GEOMAR, Kiel, 201 pp. DOI 10.3289/ifm-geomar_rep_13_2007.

Werner, R., Nürnberg, D., Hauff, F., Party, S.S.S., 2013. RV SONNE Fahrtbericht/Cruise Report SO225, Manihiki II Leg 2, The Manihiki Plateau - Origin, structure and effects of oceanic plateaus and Pleistocene dynamic of the West Pacific warm water pool ; 19.11.2012 - 06.01.2013, Suva/Fiji - Auckland/New Zealand. doi:10.3289/GEOMAR_REP_NS_6_2013, Kiel, Germany.

Willbold M, Stracke A (2006) Trace element composition of mantle end-members: Implications for recycling of oceanic and upper and lower continental crust. Geochemistry Geophysics Geosystems 7 Artn Q04004; doi: 10.1029/2005gc001005

Willbold M, Stracke A (2010) Formation of enriched mantle components by recycling of upper and lower continental crust. Chem Geol 276(3-4):188-197 doi:10.1016/j.chemgeo.2010.06.005

Winterer, E.L., Lonsdale, P.F., Matthews, J.L., Rosendahl, B.R., 1974. Structure and acoustic stratigraphy of the Manihiki Plateau. Deep-Sea Research, 21: 793-814.

Woodhead, J.D., Mcculloch, M.T., 1989. Ancient Seafloor Signals in Pitcairn-Island Lavas and Evidence for Large-Amplitude, Small Length-Scale Mantle Heterogeneities. Earth and Planetary Science Letters, 94(3-4): 257-273.

Zindler, A., Hart, S., 1986. Chemical Geodynamics. Ann. Rev. Earth. Planet. Sci., 14: 493-571.

Figure captions

Fig. 1. Bathymetric map of the Manihiki Plateau and sample locations.

Green diamonds denote locations at which high-Ti rock series and red circles low-Ti rock series were sampled from the Manihiki plateau basement (Clague et al., 1976; Ingle et al., 2007; Hoernle et al., 2010; Timm et al., 2011; Golowin et al., 2007a, b; this study). Locations of samples from this study are marked with black dot. Predicted global bathymetry is after Smith and Sandwell (1997). Inset map is after Timm et al. (2011).

Fig. 2. Detailed bathymetric maps of the SO225 remotely operated vehicle (ROV) profile area from profiles ROV3 and ROV4 and photographs of the seafloor taken during ROV sampling.

a - Bathymetric map of the boundary between the North and Western Manihiki Plateaus produced by multi-beam mapping during R/V SONNE SO193 and SO225 expeditions (Werner et al., 2013); b - Detailed bathymetry of sampled tectonic block with locations of ROV3/4 profiles and dredge SO193-DR46; c, d, e - Photographs taken during ROV Kiel 6000 dives: c - Typical rock outcrop partly covered by unconsolidated sediments and dissected by slope parallel fracture (6°04.16´S, 164°41.29´W; 3960 m.b.s.l.), d - Large debris blocks on the see floor (6°04.12´S, 164°41.25´W, ~ 4000 m.b.s.l.), e - Sample SO225-ROV3-10 in the ROV manipulator (6°04.30´S, 164°41.37´W, 4112 m.b.s.l.).

Fig. 3. Petrographic features of studied high-Ti Manihiki samples. a - Microdolerite sample SO225-ROV3-6 (optical image, crossed polarizers). The sample is largely composed of plagioclase and hornblende. b - Ilmenite partially replaced by titanite, which contains tiny zircon inclusions from sample SO225-ROV3-6 (BSE image). c - *Cpx-Pl*-phyric basalt sample SO225-ROV4-17 (optical image, crossed polarizers). d - Microcrystalline *Cpx-Pl* pyric (?) basalt – sample SO225-ROV3-11 (optical image, crossed polarizers). e. Medium-grained part

of *Hbl*-gabbro SO225-ROV3-4 (optical image, polarized light). f - Fragment of Hbl-gabbro SO225-ROV3-4 (BSE image). g - Greenschist sample SO225-ROV4-14. The rock is composed of plagioclase, chlorite and actinolite; black spots are hematite (optical image, polarized light). h - *Ol*-dolerite sample SO193-DR46-1 (optical image, crossed polarizers). i - Typical *Cpx*-*Pl*-phyric basalt of the high-Ti series - sample SO225-DR9-1 (optical image, crossed polarizers). Mineral abbreviations: *Hbl*- hornblende, *Act* – actinolite, *Pl* – plagioclase, *Tnt* – titanite, *Ilm* – ilmenite, *Zrn* – zircon, *Ap*- apatite, *Chn* – chlorite, *Ep* – epidote.

Fig. 4. Composition of amphibole. Al and Ti concentrations are in atoms per formula units (a.p.f.u.). Compositional fields of magmatic amphibole from basaltic andesites (BA), andesites (A), dacites (D), rhyodacites (RD) and rhyolites (R) are after Gillis and Meyer (2001). Pressure and temperature parameters are estimated using coexisting hornblende and plagioclase (see text). Relic high-Ti amphibole from *Hbl*-gabbro has magmatic origin; low-Ti amphiboles from studied samples are of metamorphic origin.

Fig. 5. Effect of post-magmatic alteration on major and trace element composition of Manihiki rocks. New SO225 ROV and dredge (DR) samples belong to the high-Ti group of Manihiki rocks. Major elements and LOI (loss on ignition) in wt%. $Ce/Ce^{*}=Ce_N/(La_N{*}Nd_N)^{0.5}$, where subscript "n" refers mantle-normalized values (McDonough and Sun, 1995). Literature data is after (Jackson et al., 1976; Ingle et al., 2007; Hoernle et al., 2010; Timm et al., 2011; Golowin et al., 2017a,b). Sharp changes in rock geochemistry occur at LOI exceeding 5 wt%, which is used in this study as threshold value to screen out strongly altered rocks.

Fig. 6. Major and compatible trace element composition of high-Ti samples obtained during the SO225 expedition. Samples collected with ROV are shown with green circles.

Petrographically and geochemically distinct rocks from the ROV profile are shown with different symbols: star - greenschist sample SO225-ROV4-14, crossed circle – hornblende gabbro sample SO225-ROV3-4, dotted circle - depleted sample SO225-ROV4-11. Hi-Ti Manihiki rocks from the literature (open circles) and low-Ti Manihiki rocks (small crosses) are from Ingle et al., 2007; Hoernle et al., 2010; Timm et al., 2011; Golowin et al. 2017a,b). OJP rocks (orange dots) are after Mahoney et al., 1993; Tejada et al., 1996; 2002; Fitton and Godard, 2004. Major element data were normalized to 100% on a volatile-free basis. Kroenke (Kn), Kwambaita (Kw) and Singgalo-type (Sg) OJP rocks have overlapping compositions in major elements and are distinguished in TiO_2 content. The trend of low-pressure fractional crystallization (thick blue line) starting from the composition of the most primitive high-Ti rock was calculated in Petrolog3 software (Danyushevsky and Plechov, 2011).

Fig. 7. Composition of ROV rock samples versus ROV and dredge sampling depths. Samples collected with ROV are shown with green circles. Petrographically and geochemically distinct rocks from ROV profile are shown with different symbols: star - greenschist SO225-ROV4-14, crossed circle – hornblende gabbro SO225-ROV3-4, dotted circle - depleted sample SO225-ROV4-11. Composition and sampling depth of dredged sample SO193-DR46-1 is after Timm et al. (2011).

Fig. 8. Primitive-mantle-normalized concentrations of immobile incompatible elements. High-Ti rock compositions collected during SO225 cruise: a – group of high-Ti rocks with $(La/Sm)_N>0.9$, b - group of more depleted rocks $(La/Sm)_N<0.9$, c - group of rocks with exotic petrography and/or geochemistry (greenschist, hornblende gabbro, strongly depleted rock), d – dredged samples. Rock compositions from this study are compared with DSDP Site 317A rocks (Hoernle et al., 2010) shown by shadowed field and with average compositions of Kroenke (Kn), Kwambaita (Kw) and Singgalo-type (Sg) OJP rocks shown by dashed lines

(Fitton and Godard, 2004; Tejada et al., 2002). Primitive mantle composition is after McDonough and Sun (1995).

Fig. 9. Nb depletion in high-Ti Manihiki magmas correlates with LREE enrichment and low εNd(t). Compositions of Kroenke (Kn), Kwambaita (Kw) and Singgalo-type (Sg) OJP rocks are after (Fitton and Godard, 2004; Tejada et al., 2002), low-Ti Manihiki basalts with LOI<5% (Golowin et al., 2017a). $Nb/Nb^*=Nb_N/(Th_N*La_N)^{0.5}$. Normalization to primitive mantle (McDonough and Sun, 1995).

Fig. 10. Sr-Nd-Pb isotope composition of high-Ti Manihiki rocks.

All measured isotope compositions were corrected to initial ratios assuming an eruption age of 120 Ma. Data for SO193 dredge samples are from (Timm et al., 2011). Sr and Nd compositions for DSDP Site 317A basalts are after (Hoernle et al., 2010), Pb isotopes from this study. Isotope compositions of Kroenke/Kwaimbaita- and Singgalo-type basalts are plotted based on data from (Tejada et al., 2002; 2004). Pacific MORB compositions (Mahoney et al., 1994; Regelous et al., 1999; Wendt et al., 1999; Castillo et al., 2000; Abouchami et al., 2000) are age-corrected assuming $^{147}Sm/^{144}Nd=0.25$, $^{87}Rb/^{86}Sr=0.005$, $^{238}U/^{204}Pb=10$, $^{235}U/^{204}Pb=0.073$, $^{232}Th/^{204}Pb=40$). Koolau and Pitcairn lava fields are after (Woodhead and Mcculloch, 1989; Lassiter et al., 1998; Tanaka et al., 2008) and references therein. Their compositions were age-corrected to 120Ma using parent-daughter ratios from Stracke et al. (2003).

Fig. 11. Potential temperature of Manihiki mantle sources compared to different large igneous provinces (LIPs) on Earth. All temperatures were calculated assuming accumulated fractional melting using PRIMELT3 (Herzberg, Asimow, 2015). Data for primitive rock compositions for Manihiki Plateau are from this study (high-Ti series) and Golowin et al.

(2017b) (low-Ti series). Compositions of primary melts for large igneous provinces are from compilation Herzberg and Gazel (2009), which were recalculated for the case of fractional melting in this study. The T_p range of the upper mantle is after Herzberg et al. (2007)The effect of mantle depletion (increasing source MgO) on the estimated potential mantle temperature is calculated using PRIMELT3 and parametrization from Herzberg (2004b).

Figure 1

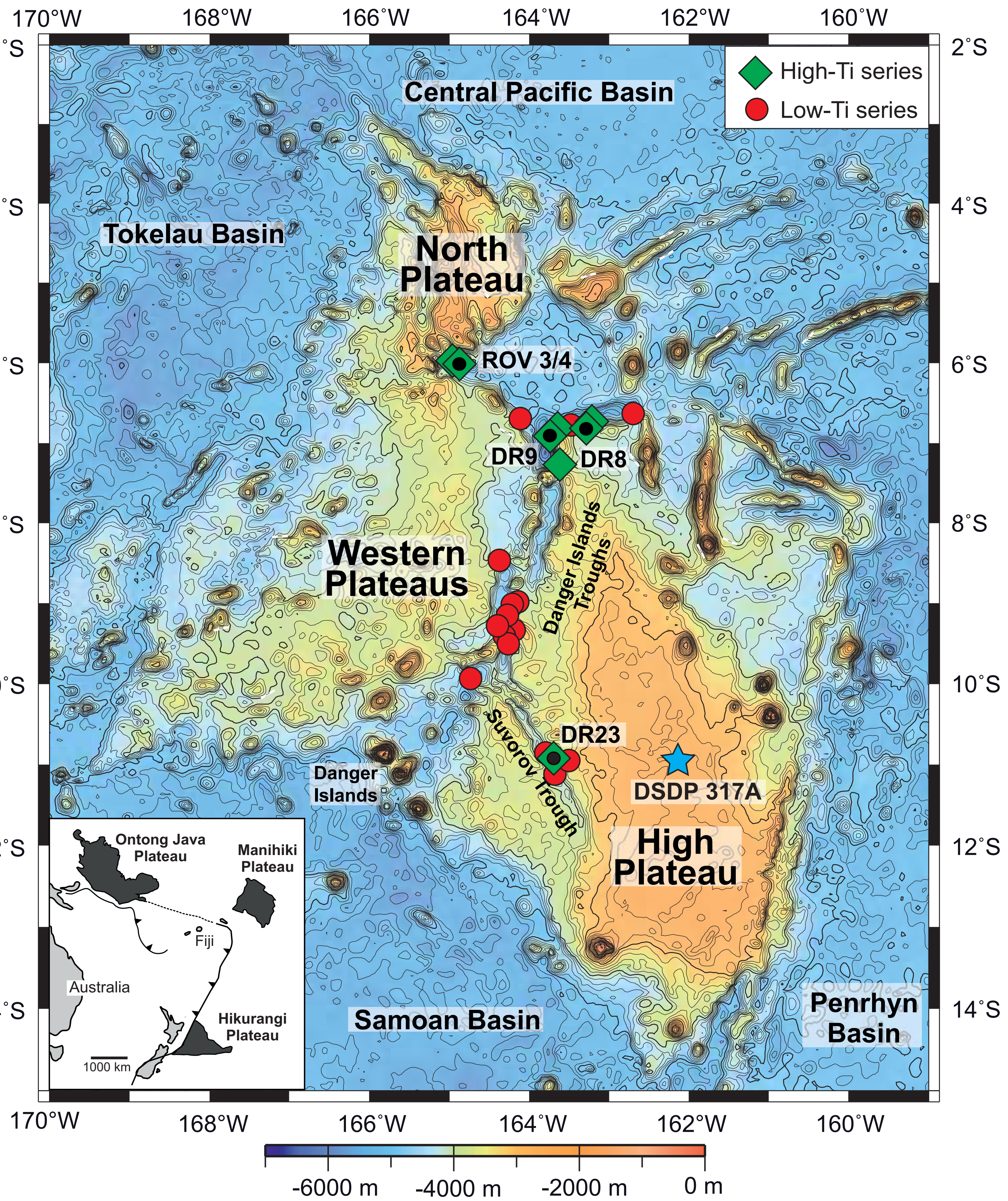

Fig. 1 (1.5 columns)

Figure 2

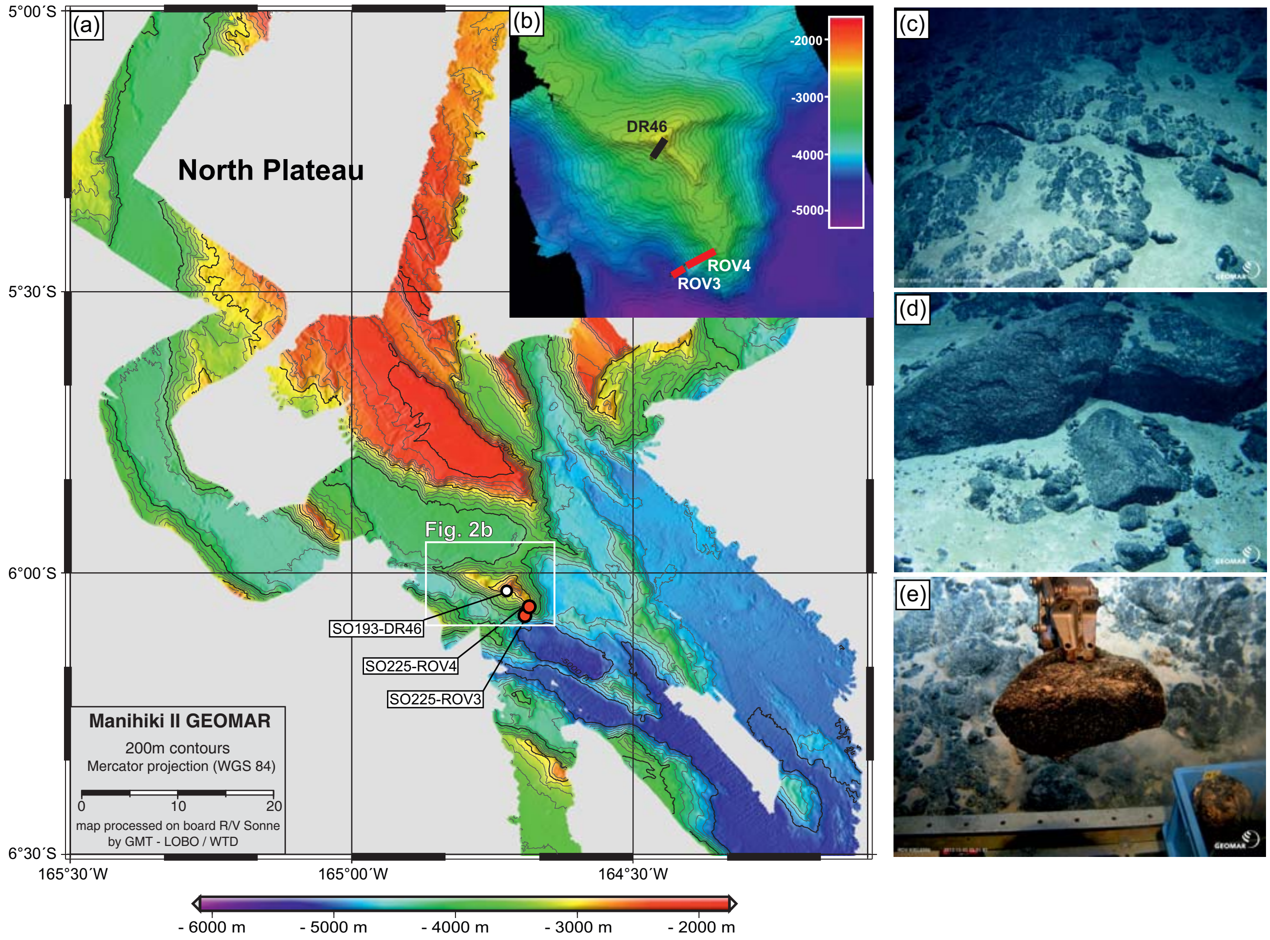

Fig. 2 (1 column)

Figure 3

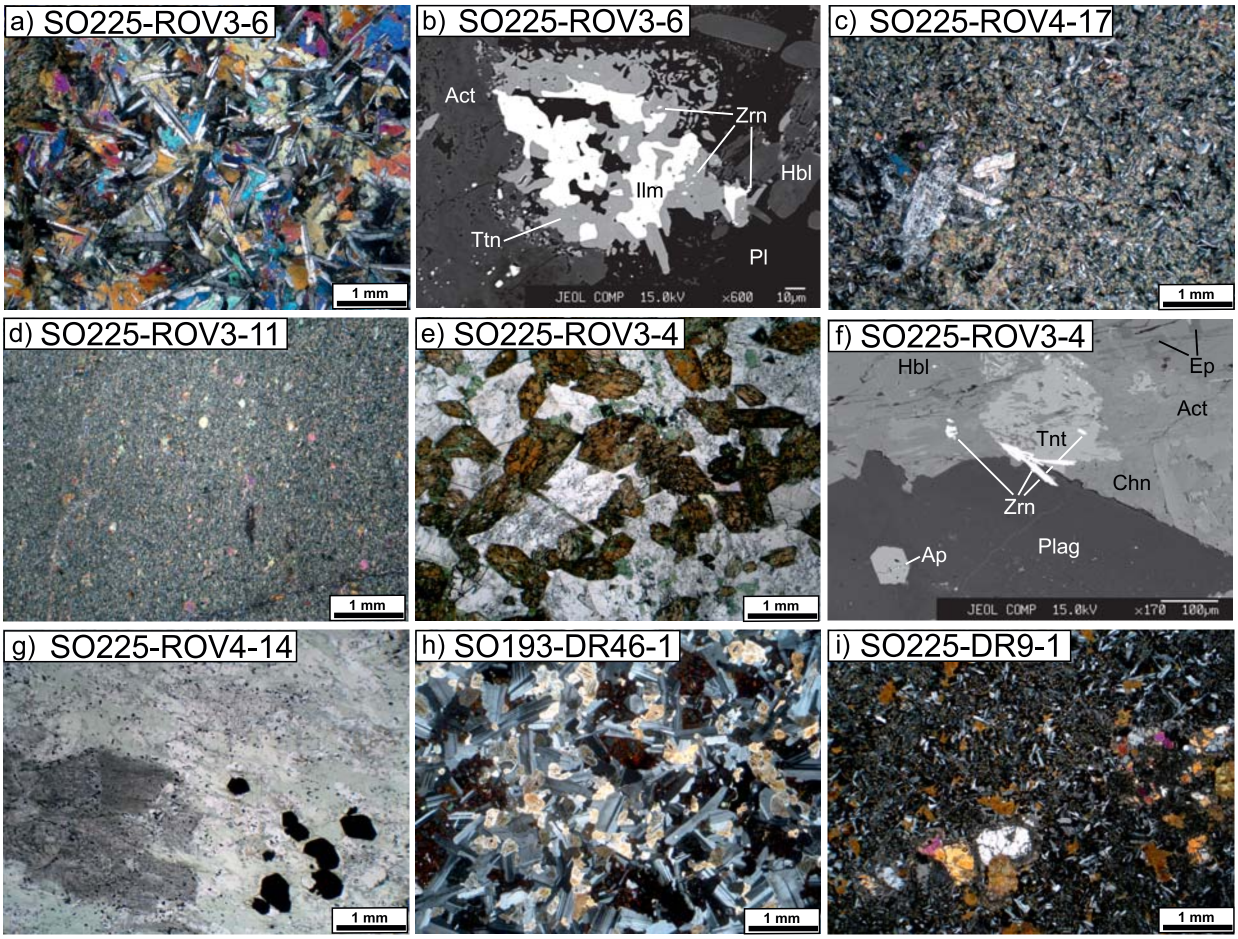

Fig. 3 (2 columns)

Figure 4

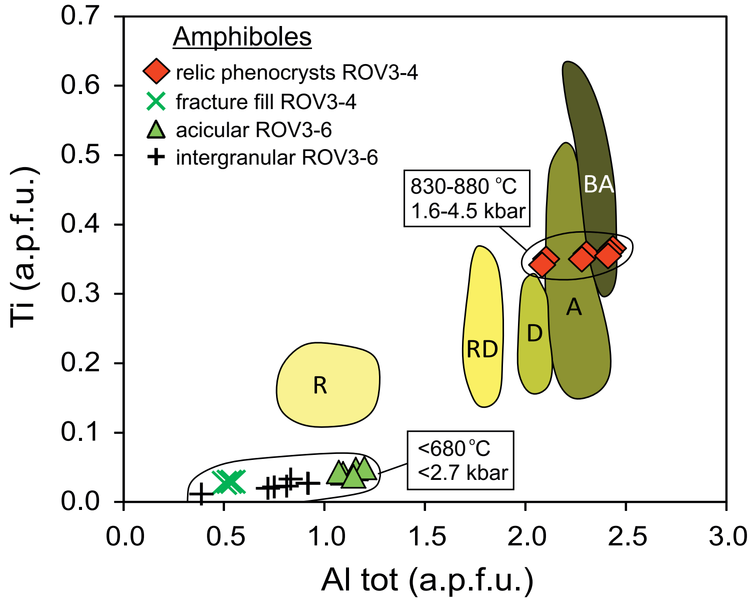

Fig. 4 (1 column)

Figure 5

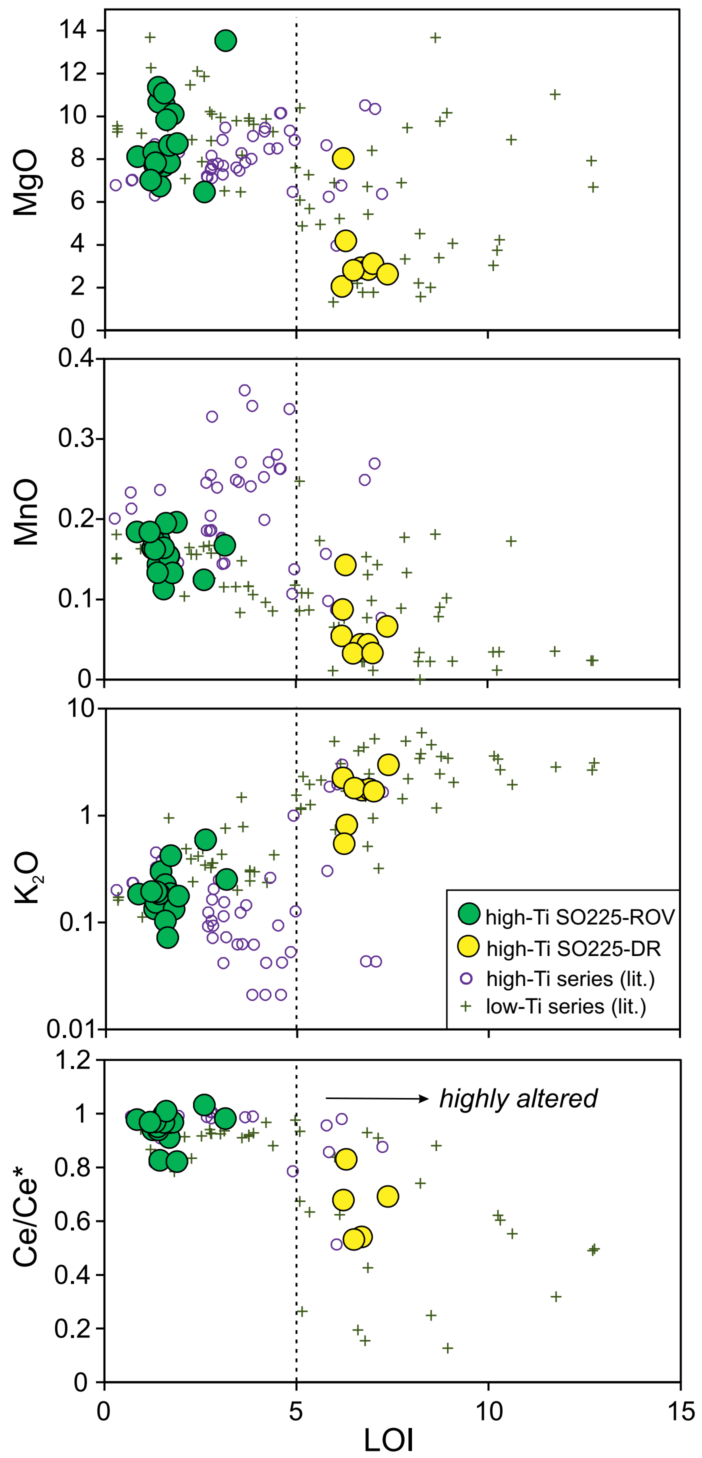

Fig. 5 (1 column)

Figure 6

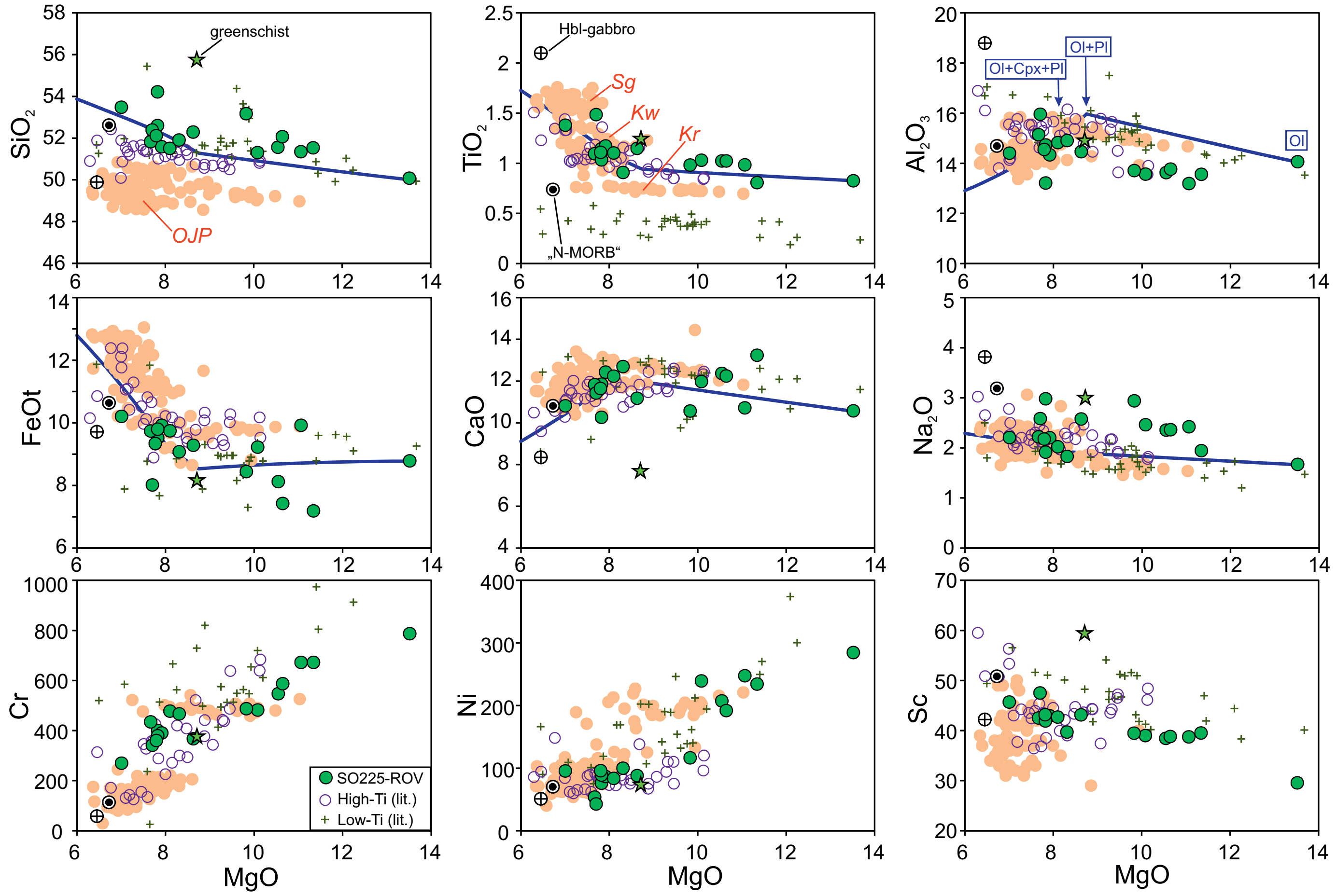

Fig. 6 (2 columns)

Figure 7

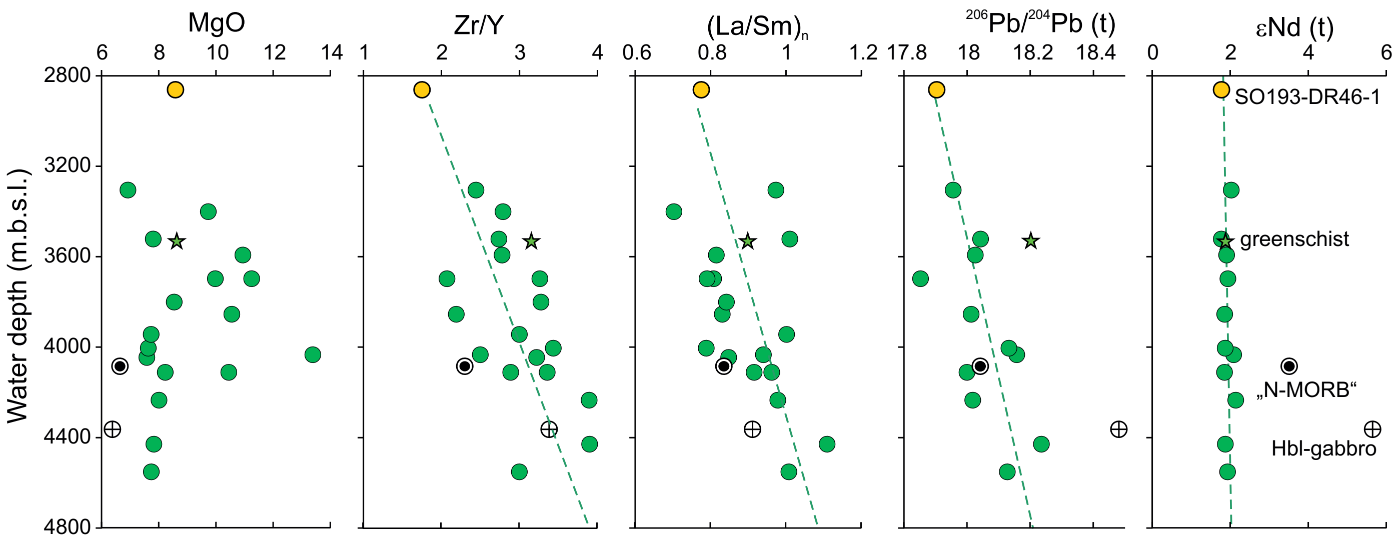

Fig. 7 (2 columns)

Figure 8

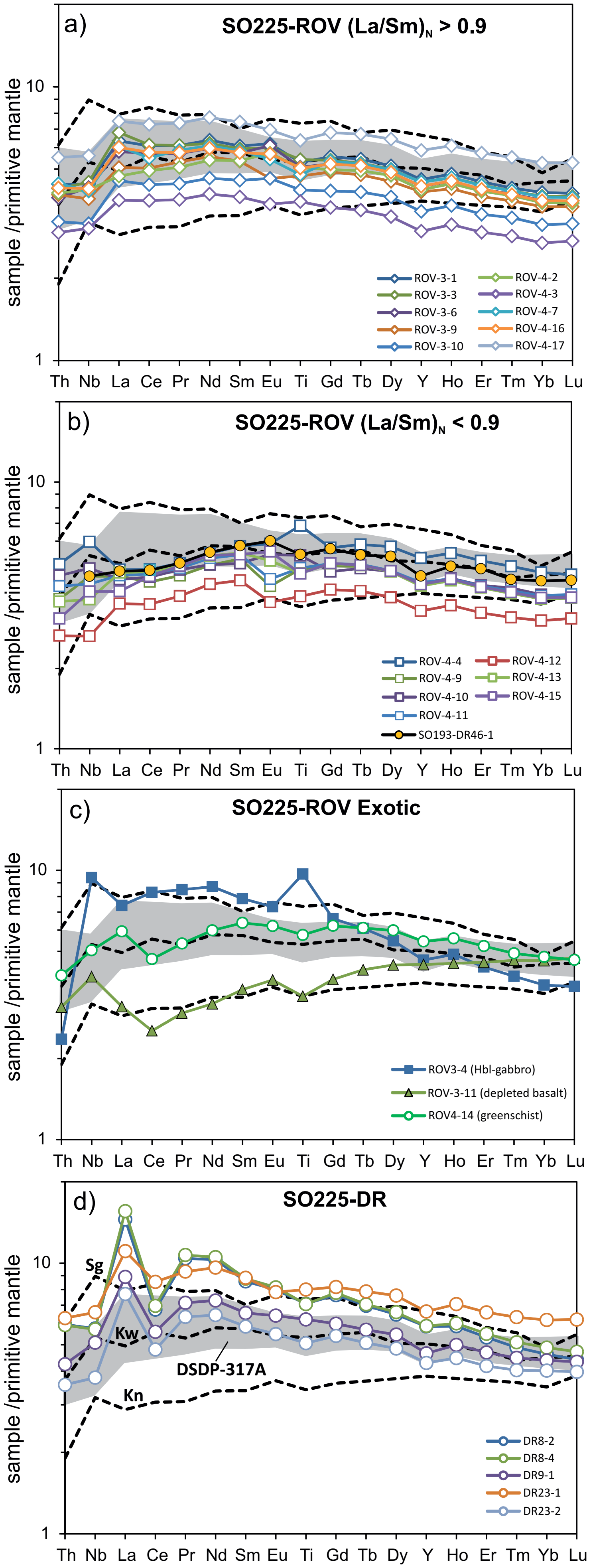

Fig. 8 (1 column)

Figure 9

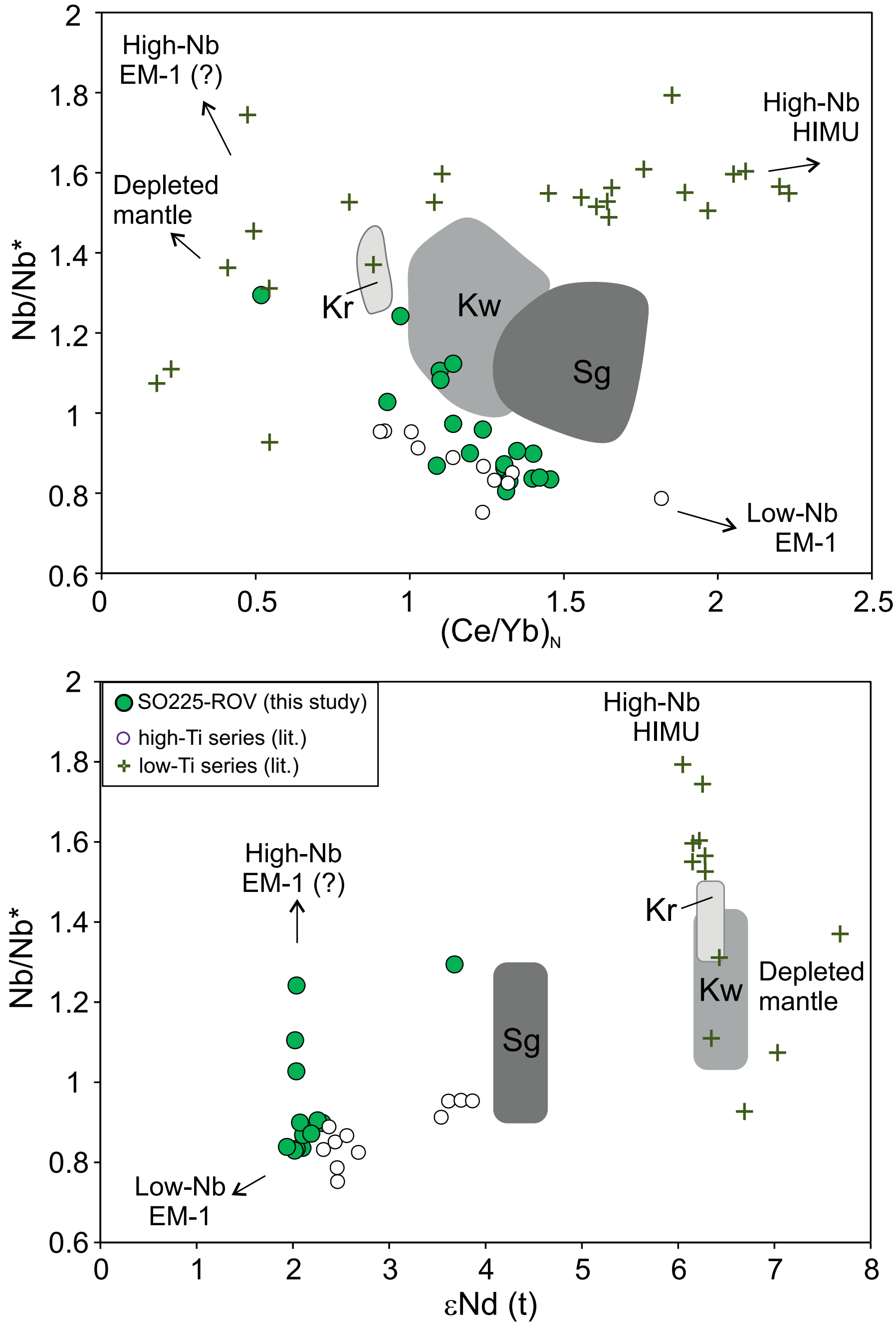

Fig. 9 (1 column)

Figure 10

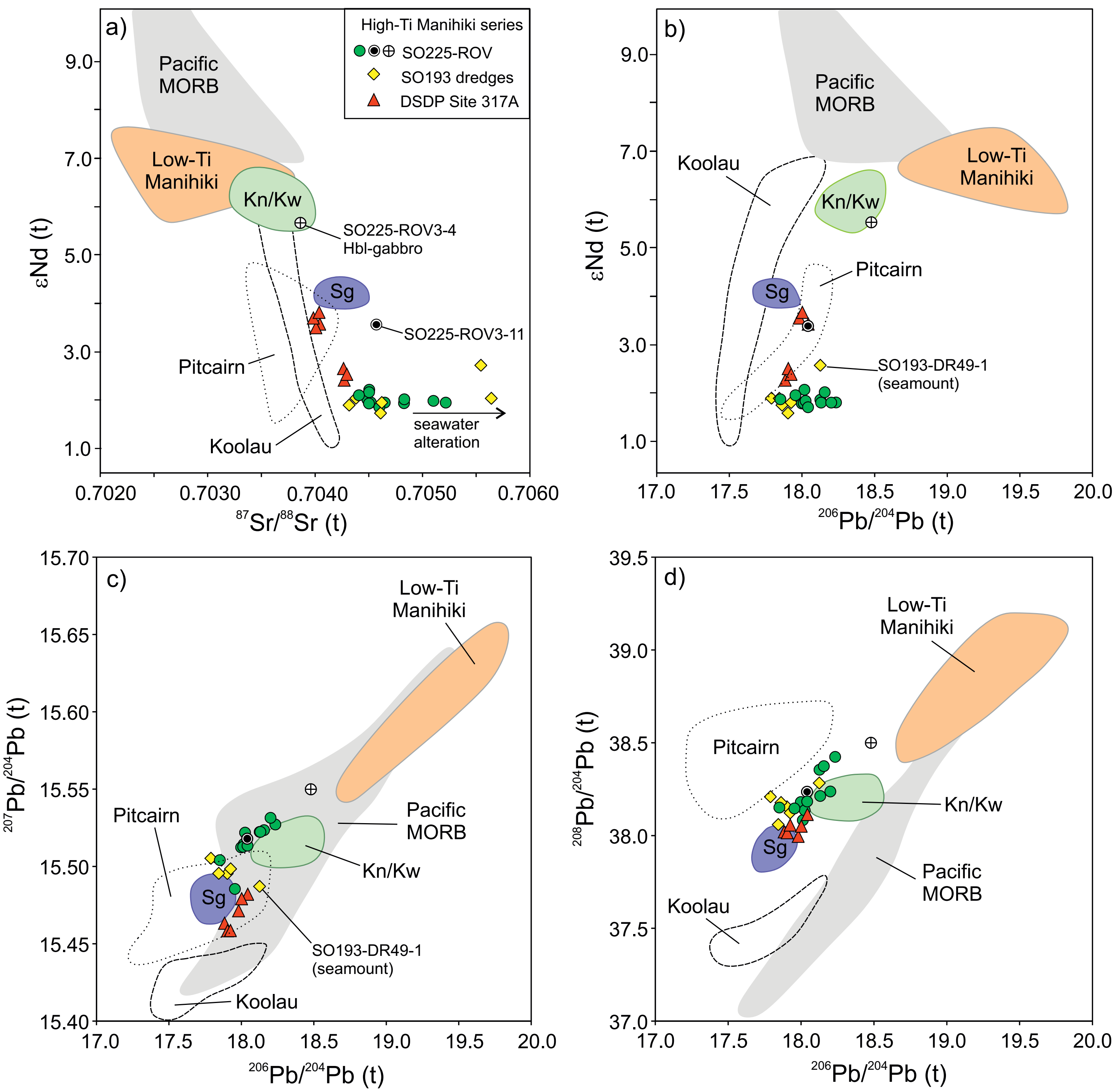

Fig. 10 (2 columns)

Figure 11

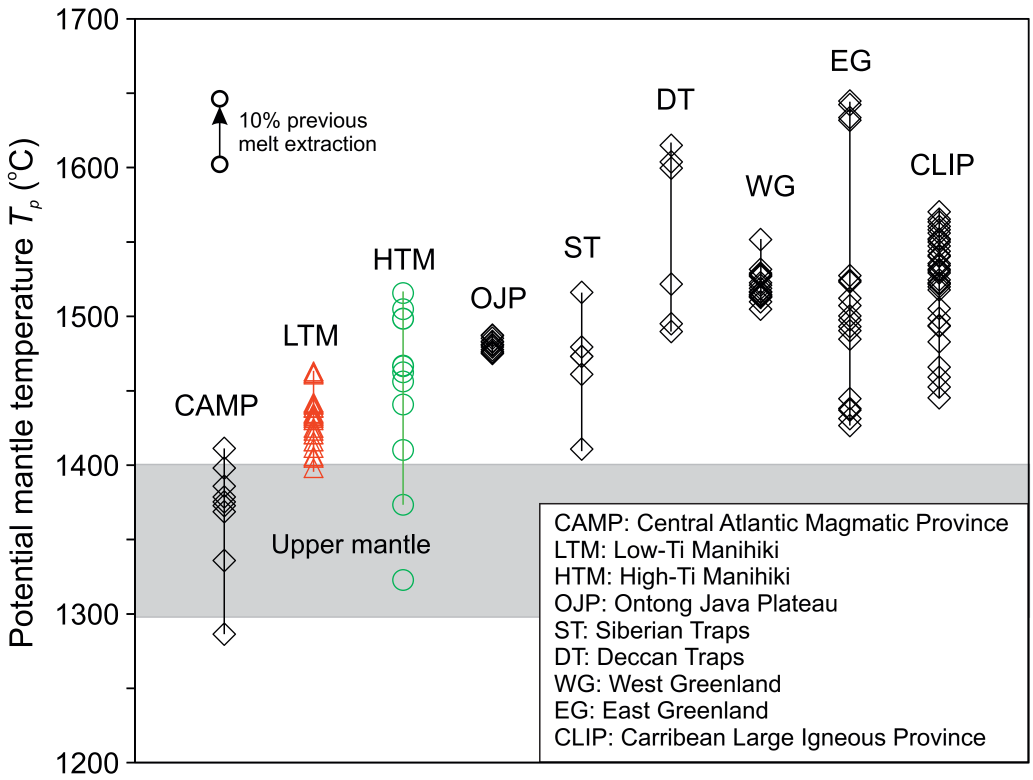

Fig. 11 (1 column)

Supplementary Methods

Click here to download Background dataset for online publication only: Supplementary methods_NEW.docx

Table S1

Click here to download Background dataset for online publication only: Supplemenrary table 1(wr xrf-icpms).xlsx

Table S2

Click here to download Background dataset for online publication only: Supplemenrary table 2 (wr Sr-Nd-Pb isos).xlsx

Table S3

Click here to download Background dataset for online publication only: Supplementary table 3 (Minerals).xlsx

Table S4

Click here to download Background dataset for online publication only: Supplementary table 4 (PRIMELT).xlsx